

RESEARCH ARTICLE OPEN ACCESS

SARchaeological Prospection: Synthetic Aperture Radar for the Reconstruction and Mapping of Temperate Floodplain Environments

Nicholas Crabb¹  | Chris Carey¹  | Andy J. Howard²  | Matthew Brolly³ 

¹Department of Archaeology and Anthropology, Faculty of Science and Technology, Bournemouth University, Poole, UK | ²Landscape and Research Management, Bridgnorth, UK | ³Centre for Earth Observation Science, University of Brighton, Brighton, UK

Correspondence: Nicholas Crabb (crabbn@bournemouth.ac.uk)

Received: 18 January 2025 | **Revised:** 29 May 2025 | **Accepted:** 3 June 2025

Funding: This work was supported by the UK Research and Innovation (EP/L016036/1).

ABSTRACT

Temperate river floodplains present a significant challenge for archaeologists, as cultural and palaeoenvironmental remains are often difficult to locate but can be exceptionally well preserved, especially where groundwater levels are high. In these alluvial environments, the deposition of thick, fine-grained sediments has potential to deeply bury rich archaeological archives that can be used to reconstruct past environments, but these deposits also render conventional forms of archaeological prospection largely ineffective. Consequently, subsurface mapping techniques have been developed to determine the three-dimensional spatial distribution of archaeological remains and their relationship to sediment architecture within alluvial environments. These can be generated using a combination of intrusive (boreholes, trial pits, etc.) and nonintrusive (e.g., geophysical survey) investigations augmented by other geological and topographical datasets. Although lidar and other passive remote sensing methods such as multispectral imagery and aerial photography have been utilized to investigate floodplain landscapes, the spaceborne capabilities of Synthetic Aperture Radar (SAR) have yet to be explored within the context of geoarchaeological prospection. This contribution, therefore, examines the capacity of SAR to reconstruct and map landform assemblages within temperate river floodplains by analysing images in a 6-year time series of (COSMO-SkyMed) SAR data across two valleys in Herefordshire, United Kingdom. The results demonstrate that SAR can be used to record the spatial extent of recent flood events to outline surface topographic complexity and water table levels to achieve a detailed understanding of subsurface complexity across temperate river floodplains. This information can, in turn, be used to form a ‘model’ of the likely distribution and potential preservation conditions of archaeological resources. Although higher resolution topographic datasets (e.g., lidar, if available) may often be more effective, the integration of SAR within geoarchaeological investigations provides an alternative data source for the reconstruction of alluvial landscapes.

1 | Introduction

Temperate river valleys have provided resource-rich locations for a wide range of past human endeavours, including from later prehistory, settlement, ritual and funerary activity (Booth et al. 2007; Brunning and Chapman 2013; Lambrick et al. 2009; Morigi et al. 2011). Evidence for this activity is often visible

and densely clustered upon late Pleistocene river terraces and gravel islands both within and at the margins of postglacial valley floors, which, in contrast, are often characterized by a dearth of visible archaeology (Bradley 2012; Evans, Tabor, and Vander Linden 2016; Hosfield and Green 2013; Van de Noort and O’Sullivan 2006; White et al. 2016). The settlements and monuments on the terraces and gravel islands are generally visible

This is an open access article under the terms of the [Creative Commons Attribution](https://creativecommons.org/licenses/by/4.0/) License, which permits use, distribution and reproduction in any medium, provided the original work is properly cited.

© 2025 The Author(s). *Archaeological Prospection* published by John Wiley & Sons Ltd.

because the soils are thin and dry, and the identification of archaeological sites is conducive to a range of well-established prospection techniques such as aerial photographic analysis, fieldwalking, shallow geophysical survey, trial trenching and test pitting. In contrast, contemporary, postglacial valley floors, especially in lowland and perimarine environments, can contain thick > 1 m (Holocene) alluvial sedimentary sequences (Carey et al. 2006; Guccione 2008; Howard et al. 2008; Meylemans et al. 2013; Passmore, Waddington, and Houghton 2002). These have the potential to mask archaeological resources and render most conventional forms of archaeological prospection ineffective (i.e., those described previously). Yet, despite this, the high-water tables and associated anoxic conditions found within floodplains can lead to exceptional levels of preservation of both cultural and palaeoenvironmental material (Hill 2014; Matthiesen et al. 2022). Consequently, temperate floodplain landscapes are rewarding but highly challenging to investigate, and archaeologists must understand the geomorphology of these landscapes to understand the distribution of archaeological resources.

Temperate alluvial environments contain assemblages of landforms that provide records of the evolution of river systems (e.g., terraces, palaeochannels and other bedforms; Brown 1997). The stratigraphy of alluvial sediments also represents a chronological sequence, the analysis of which can provide information regarding past environments, climate and vegetation histories (Historic England 2018). As the presence and likely preservation of archaeological and palaeoenvironmental material vary according to the distribution and type of different landforms, defining the morphology and sedimentary sequences of alluvial environments is imperative for understanding the distribution of archaeological resources. As a result, archaeologists identify, and map, buried landforms to determine zones of archaeological and palaeoenvironmental preservation potential. However, most of these investigations rely on traditional (intrusive) datasets (e.g., boreholes and test pits), which can be costly and impractical to implement within large-scale landscape analyses. Many investigations also integrate geotechnical logs, which may not be sufficiently detailed or well positioned for archaeological purposes. As these datasets are ordinarily sparsely distributed points in a landscape, the results are often presented in an interpolated format (model), which, although extremely useful for interpretation, can miss features or landforms of interest. More recently, however, remote sensing data are increasingly integrated within these investigations to fill these gaps and aide the identification of archaeologically significant landforms.

This paper provides an examination of the capacity of Synthetic Aperture Radar (SAR) to reconstruct and map archaeological resources within temperate river floodplains. Although lidar and other passive remote sensing methods (e.g., multispectral imagery and aerial photographs) have been utilized to investigate floodplain landscapes, advancements in the spaceborne capabilities of SAR have yet to be explored within this context. As such, this paper establishes a novel approach to summarizing relevant information from a SAR time series and considers the contribution this can make to geoarchaeological models of temperate river floodplains. Such investigations into the capacity of nonintrusive (remote sensing) methods are critical to heritage professionals working in alluvial environments, particularly

ahead of any potential threats to these resources such as through infrastructure development and aggregate extraction, which are common in river valley settings (Kibblewhite, Tóth, and Hermann 2015), or flood alleviation and natural flood prevention schemes (Boardman and Boardman 2024; Carmichael et al. 2023; Howard et al. 2017). As climate change is predicted to increase the intensity and frequency of rainfall, causing unspecified changes in ground conditions, that will affect the preservation of archaeological resources (Fluck and Dawson 2021), the ability to understand the subsurface complexity of alluvial environments using methods that are more compatible with broader values of sustainability, such as remote sensing data, is of increasing importance.

1.1 | Understanding Subsurface Complexity in Temperate Floodplain Environments

The main aim of geoarchaeologists working in temperate floodplain environments is to locate areas of greatest archaeological potential. This is normally achieved through the recording of subsurface sediments and stratigraphy, to characterize variation in deposits attributable to environmental and geomorphological processes, which, in turn, inform an understanding of the preservation potential of archaeological remains (Carey et al. 2018). Such an approach is otherwise known as ‘deposit modelling’, which provides a framework for understanding the distribution of complex (often deep) depositional sediment sequences, typically comprising a visual representation of spatial and stratigraphic relationships between natural subsurface sediments, palaeoenvironmental remains and archaeological features (Carey et al. 2019; Historic England 2020). This can vary from two-dimensional vertical cross-sections and horizontal surfaces to deposit thickness maps (Bruniaux et al. 2024) and pseudo-three-dimensional models (Carey et al. 2018; Champness 2018). Regardless of their visual output, deposit models are typically constructed through the combined analysis of existing records (e.g., topographic and geological mapping, geotechnical logs and Historic Environment Record [HER] data) and intrusive investigations, such as boreholes, coring, trial trenching or excavation (Ayala et al. 2017; French et al. 2005; Houben et al. 2013). Deposit models are, therefore, inherently grounded in conventional archaeological and geomorphological approaches (primarily stratigraphic analysis), but they can incorporate data from disparate, albeit complementary, methods that provide direct and proxy measurements of the subsurface (Carey et al. 2019).

Understanding the complexity of temperate floodplain environments is not restricted to the use of ‘intrusive’ datasets, which can be costly and impractical to acquire across large areas. Numerous studies have, therefore, integrated geophysical survey (Bates and Bates 2016; Engel et al. 2022; Verhegge, Missiaen, and Crombé 2016; Verhegge et al. 2021) and remote sensing data (Berendsen, Cohen, and Stouthamer 2007; Berendsen and Volleberg 2007; Carey et al. 2006; Challis, Carey, et al. 2009; Jones et al. 2007; Malone 2014; Stein et al. 2017; van Dinter et al. 2017), which have shown enormous potential to enhance the understanding of the distribution of archaeological resources within a variety of complex depositional environments. In particular, the widespread (national) collection of lidar data by the Environment Agency in England (and other government

organizations globally) has revolutionized the mapping of landform assemblages (Chiverrell, Thomas, and Foster 2008; Jones et al. 2007; van der Meulen et al. 2020). More specifically, in the context of deposit models, lidar data provide a valuable topographic and stratigraphic control from the contemporary ground surface downwards (Crabb et al. 2023). However, this can be less effective in river systems where channels have remained stable in the mid-late Holocene and vertical accretion has dominated, thereby blanketing and smoothing floodplain topography (Howard et al. 2015). Thus, it is beneficial to integrate other remote sensing datasets that may allow for additional landforms with a high potential to provide additional geoarchaeological information but are not expressed topographically, to be identified.

The utilization of aerial imagery to map surface landform assemblages within river floodplains for both archaeological (Baker 2003, 2007; French, Macklin, and Passmore 1992; Lambrick 1992) and geomorphological (Fezer 1971; Jensen 2007; Pouquet 1974; Rosenfeld 1984; Short and Blair 1986) investigations is an established methodology. Advancements in sensor technology, digital image processing and increased computational power over the last two decades has led to the integration of a wider suite of remote sensing datasets for the study of alluvial environments (Lillesand, Kiefer, and Chipman 2015, Chapter 2). For example, Challis, Kinsey, and Howard (2009) exemplified the potential of airborne multispectral and hyperspectral imaging for the investigation of valley floor geoarchaeology, although the cost and mobility of these airborne systems were a significant barrier to their wider adoption and there is now more limited access to such resources following the closure of the NERC Airborne Research Facility. Similarly, the use of airborne SAR has been hampered by prohibitive costs and the low spatial resolution for archaeological purposes, which has led to SAR data being largely overlooked as a tool for research by the archaeological community. Despite this, SAR is increasingly utilized in other disciplines to study aspects of alluvial environments such as monitoring river channel changes (Mitidieri et al. 2016; Nagel, Darby, and Leyland 2023; Rossi et al. 2023), erosion (Freihardt and Frey 2023), sediment accumulation (Hachemi et al. 2021) and flood mapping (Amitrano et al. 2024; ESRI 2024; Grimaldi et al. 2020). This has been facilitated by the increased resolution and improved accessibility (and density) of image archives and tasking opportunities provided by contemporary higher resolution SAR systems and has also led to an increase in archaeological explorations of this technology (Cigna et al. 2023). Therefore, SAR data have considerable potential to aid alluvial geoarchaeological investigations, but this has yet to be fully realized.

2 | SAR Earth Observation

SAR is an active remote sensing method commonly deployed on spaceborne platforms for imaging. The basic operation principle is that a series of radar pulses are transmitted towards the ground surface and the time taken to receive backscattered echoes and the amplitude of that reflected signal is recorded (Chapman and Blom 2013). The amount of radar energy returned (or backscattered) to the sensor is primarily determined by the shape and orientation of the target, as well as surface roughness (Chuvieco 2020, Chapter 2). Rough terrain

scatters incident energy in multiple directions (diffuse), and smooth surfaces reflect energy away (specular) from the sensor (Simms 2020). Together with these geometric characteristics, the dielectric constant of surface features influences the intensity of the backscatter. Most natural surface materials have a dielectric constant in the order of 3–8 when dry, whereas water has a dielectric constant of 80 (Lillesand, Kiefer, and Chipman 2015, 421). As a result, soil moisture and surface wetness variations can be identified by relative increases in the backscatter record; although if the area becomes inundated, the scattering becomes specular with the recorded backscatter reducing significantly (El Hajj et al. 2016). The SAR approach to radar remote sensing allows imaging to take place at high resolution by synthesizing a large antenna, which would be practically unachievable on traditional spaceborne platforms. The synthesized antenna size is achieved by taking advantage of the relative motion of the sensor to the ground and correcting for doppler shifts to create useable imagery.

As vegetation has a high moisture content, it is a good scatterer of radar energy, although different vegetation types have different backscatter properties (Simms 2020, 90). Healthy plants have a higher water content, and thus relatively higher dielectric constant, which increases reflectivity, and the presence of extensive, complex or oriented vegetation structures can also increase radar backscatter (Santi et al. 2012). As such, there are a variety of agricultural applications of SAR for mapping crop extent, type (Blickensdörfer et al. 2022) and condition, as well as providing estimates of soil moisture and crop yield (Chang-an et al. 2019; Parag et al. 2024). However, the interpretation of vegetated areas is not straightforward, as it forms a complex heterogenous volume consisting of the plant structure, typically consisting of multiple size scatterers, and underlying soil (Jones and Vaughan 2010, 67). Despite this, the presence of large-scale archaeological features or geomorphological landforms may be apparent within SAR imagery, but this also is dependent on other SAR sensor parameters including wavelength, spatial resolution and polarization.

2.1 | SAR Sensor Parameters

2.1.1 | Wavelength

SAR operates in the microwave portion of the EM spectrum with wavelengths ranging from the metre (P Band) to centimetre scale (Ka Band). Bands are typically denoted by letters, with the most used for imaging being P, L, S, C and X giving a frequency coverage from ~0.03 to ~12 GHz. The wavelength influences how the radar signal interacts with the feature and how far a signal can penetrate the target (Figure 1). For example, radar pulses transmitted from an X-band radar, operating at a wavelength of ~3 cm (Brolly and Woodhouse 2012; Gorrab et al. 2014), produce backscatter responses mostly driven by the texture or ‘roughness’ of the surface such as that produced by surface vegetation or canopy cover (Meyer 2019). On the other hand, under the same conditions, an L-band signal, operating at a wavelength of ~20 cm, can penetrate soil and vegetation to some extent to potentially define shallow subsurface conditions with the backscatter response driven by a combination of the ‘roughness’ of the surface and characteristics of the subsurface

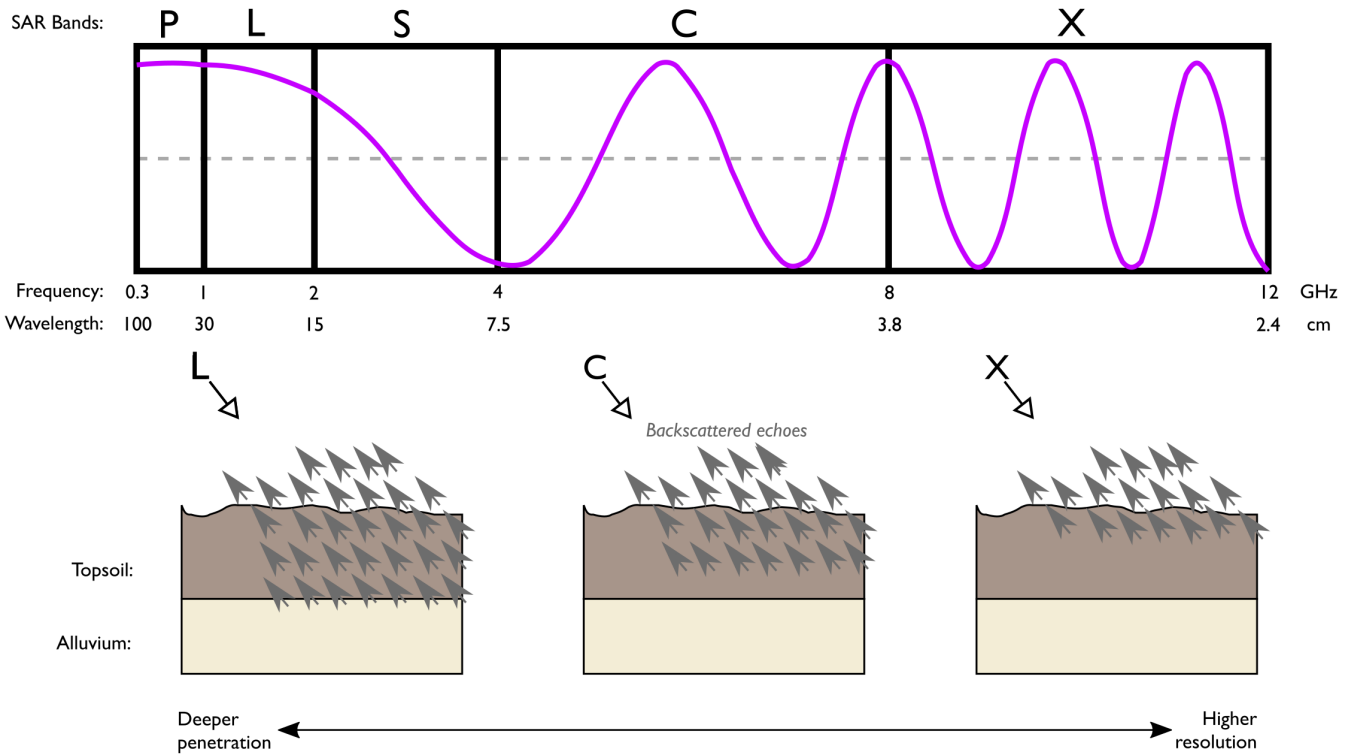


FIGURE 1 | Illustration of the relationship between the frequency and wavelength of SAR bands and the depth of penetration/spatial resolution (adapted from Meyer 2019).

such as moisture content and compactness (Luo et al. 2019). Unfortunately, however, radar pulses with longer wavelengths are typically associated with lower bandwidth SAR systems for imaging and therefore result in lower achievable spatial resolution, but because the depth of penetration using SAR sensors with longer wavelengths is still relatively minimal (e.g., L-band systems penetrate up to 24 cm in optimal dry sandy conditions such as deserts; Gorrab et al. 2014), it is arguably more important to focus on achieving better (higher) spatial resolution for (geo)archaeological purposes.

2.1.2 | Spatial Resolution and Imaging Mode

The level of detail in geophysical and remote sensing datasets is commonly referred to spatial resolution, which can be stated as the amount of ground surface area (m^2) within each pixel in an image (Campana 2017, 706). For optical sensors, spatial resolution decreases as the altitude, or distance from the ground, increases, but the spatial resolution of SAR data is best understood in terms of the range (across-track) resolution and azimuth (along-track) resolution. The range resolution is related to the bandwidth of the system, which is a system specific parameter unrelated to the wavelength. The limiting factor here is the pulse width, with shorter pulses producing higher spatial resolution, albeit at lower energy (Ager 2021). When using non-SAR radar, or ‘real aperture radar’, an impractically large antenna would be required to provide suitable azimuth resolution of earth surface targets from space or an aircraft and shorter wavelengths at closer range producing the best azimuth resolution outcomes (NASA 2024b). For SAR systems, the azimuth resolution is independent of the wavelength of the system and of the distance

between target and sensor (Hein 2003). Thus, the spatial resolution of SAR data can be considered proportional to the size of the physical radar antenna with smaller antennas allowing an increased dwell time on a target due to greater beam spreading, producing higher resolution, and the nominal azimuth resolution is that corresponding to half the physical antenna size. However, a further factor that influences the spatial resolution (and area coverage) of SAR is the imaging mode in which the data are collected (Kumar et al. 2023, chapter 1).

There are four common imaging modes for SAR; Stripmap, Spotlight, Dwell and Scan. In ‘Stripmap’ mode, radar pulses are transmitted at a fixed off-nadir angle, resulting in a medium (3- to 15-m) resolution swath of contiguous data (Khoshnevis and Ghorshi 2020). Higher (<1-m) spatial resolution data can be obtained in ‘Spotlight’ and ‘Dwell’ modes, where radar pulses are directed towards targeted areas from multiple angles for extended periods of time (Meyer 2019). This creates a higher synthetic aperture length, providing a higher resolution at the expense of area coverage. Lastly, in ‘Scan’ mode, a large swath coverage is achieved by switching the antennae look angle of the radar pulses in multiple swaths, achieving larger area coverage, but lower (30- to 100-m) spatial resolution.

2.1.3 | Polarization

The polarization of a radar signal refers to the geometric plane (orientation) in which the transmitted and/or received radar pulse oscillates (Lillesand, Kiefer, and Chipman 2015, 451). Typically, radar collects signals in different polarizations that are oriented either parallel (horizontal) or perpendicular (vertical)

to the surface target (Kumar et al. 2023). Horizontal polarization is indicated by the letter H, and vertical polarization is indicated by V, resulting in four possible polarization combinations (HH, VV, HV and VH) with the first letter representing the transmitted and the second letter the received. Several modern SAR sensors are ‘fully polarimetric’ in that they record each of these polarization combinations (Lasaponara and Masini 2013). This can be beneficial as different polarizations respond differently to the distinct types of surfaces. For example, rough surfaces, such as that caused by bare soil or water, are most sensitive to VV scattering, whereas double-bounce scattering typically caused by buildings/tree trunks is most sensitive to an HH polarized signal (Meyer 2019). HV is used to indicate depolarizing surfaces such as vegetation canopies where volume scattering occurs. It has been suggested that VV polarizations are most suitable for palaeolandscape features (Elfadaly et al. 2020), but there is currently little consensus in the literature with regard to which is the most effective polarization mode for archaeological research (Chen et al. 2022).

2.2 | SAR in Archaeological Research

SAR systems have been employed since the 1980s for a variety of archaeological purposes (Adams, Brown, and Culbert 1981; Blom, Crippen, and Elachi 1984; Chen, Jiang, et al. 2017; Conesa et al. 2014; Dore et al. 2013; Garrison et al. 2011; Kiarszys and Zalewska 2017; McHugh et al. 1989; Moore, Freeman, and Hensley 2007). Initially, the application of SAR was focused on detecting shallow subsurface features, predominantly in desert regions, by exploiting the capability of long wave (L-band) systems to penetrate dry sand and detect relatively large buried features (Holcomb and Shingray 2007; Wiseman and El-Baz 2007). It has also been used successfully in vegetated areas, though the subsurface imaging capability is negligible where dense vegetation cover is present (Stewart 2017). However, SAR is perhaps mainly utilized for detecting upstanding or microrelief remains (e.g., earthworks or structural remains; Chen et al. 2016; Haskins 2010; Patruno et al. 2013; Tapete and Cigna 2017).

Most archaeological applications of SAR have used Normalised Radar Cross Section, also known as σ^0 , or backscatter (Lasaponara and Masini 2013), which provides information about surface characteristics according to the wavelength frequency, polarization and incidence angle, to detail buried features, as well as extant remains such as earthworks, walls and other structures (Luo et al. 2019). Backscatter anomalies can be caused by archaeological features under vegetation/crops and bare soil, due to variations in sediment composition, density and texture, and the dielectric constant and moisture content of different materials (Jiang et al. 2017; Tapete and Cigna 2017). Thus, with the appropriate selection of imaging mode, together with favourable environmental conditions (e.g., soil moisture and vegetation coverage), information relating to the presence of archaeological features and alluvial landforms can be acquired (Chen et al. 2015). Despite this potential and reviews outlining its value for archaeology (Chen, Lasaponara, and Masini 2017; Lasaponara and Masini 2013; Tapete and Cigna 2017, 2019), SAR is less frequently used than lidar or passive methods, primarily because the spatial resolution of the imagery is considered to be too coarse to adequately define small archaeological

features (Tapete and Cigna 2019). However, modern X-band systems (e.g., TerraSAR-X/TanDEM-X and COSMO SkyMed) are better suited to the study of archaeological sites, despite their limited surface penetration, due to their higher spatial resolutions achieved through higher bandwidth and smaller antennas (Dore et al. 2013; Erasmi et al. 2014; Lasaponara and Masini 2013; Tapete and Cigna 2019). For example, COSMO SkyMed operates with a maximum bandwidth of 400 MHz and antenna length of 5.7 m, whereas the ALOS PALSAR 2 L-Band system operates with a maximum bandwidth of 84 MHz and antenna length of 10 m, which results in larger resolution cells.

A further benefit of modern SAR systems to archaeological research is the short revisit times and an increasing availability of historical archives of data (Cigna et al. 2014). This is advantageous as this ‘timeseries’ of data can enable change detection of features and help with monitoring the condition of cultural heritage sites. This can be achieved using interferometry, which requires imaging the same location from different angles to analyse phase changes between two images to infer elevation changes (Chen, Lasaponara, and Masini 2017). Collecting multiple SAR images over the same area at different times may also lead to speckle reduction through temporal averaging (Tapete and Cigna 2019). Interferometry also enables a single image to be produced, representing the temporally averaged backscattering signal, which retains the spatial resolution of the input scenes and provides an enhanced level of detail, so that features unchanged throughout the time series are better imaged and resolved (e.g., Cigna et al. 2014). Thus, an extensive time series of SAR data greatly improves the quality of information and the potential for extracting small-scale features (Stewart 2017) and can allow for the monitoring of impacts to heritage sites (Tapete, Cigna, and Donoghue 2016). These time series also have potential to delineate subsurface geomorphological landforms within river floodplains through the analysis of backscatter changes, but this has yet to be explored in an archaeological context.

3 | Regional Setting of the Case Studies

The main aim of this research was to examine the capacity of SAR to reconstruct and map archaeologically significant landform assemblages within temperate river floodplains and, therefore, assess the potential of SAR to contribute to the construction of geoarchaeological deposit models. To achieve this, it was necessary to acquire datasets from typical temperate river floodplain settings and two case study areas were investigated in Herefordshire, United Kingdom (Figure 2). These were selected as each floodplain records aspects of landscape evolution that are likely to have influenced the distribution of cultural and environmental material. More specifically, the lower part of River Lugg and the middle portion of the River Wye valleys were selected as they represented typical temperate river floodplains with a variable level of prior archaeological research across (Watt 2011).

3.1 | Lower Lugg Valley

The Lower Lugg valley is in the centre of Herefordshire and covers a 10×6 km area, extending from Dinmore Hill to northeast

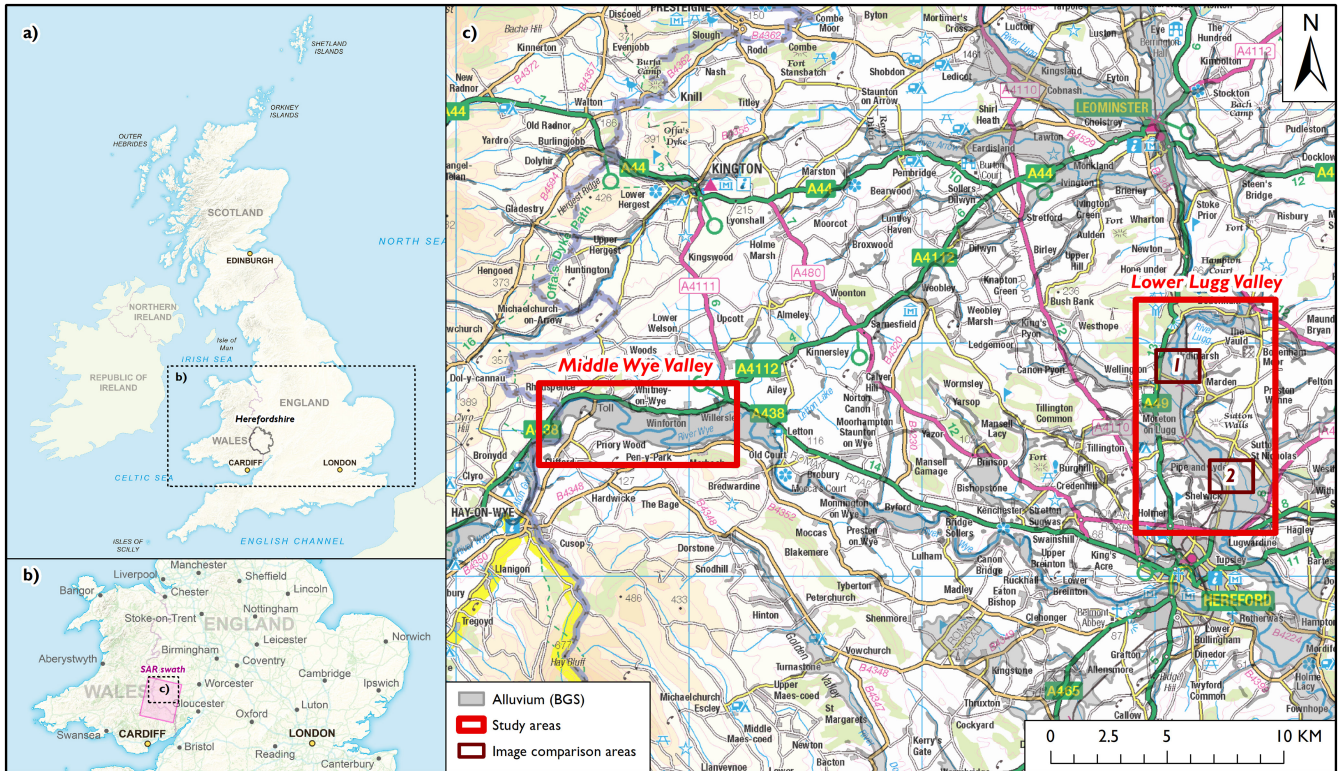


FIGURE 2 | Location of study areas on a national and regional scale (a, b) with the extent of floodplain covered in relation to mapped (British Geological Survey) alluvial deposits (c).

of the city of Hereford. It is characterized by a broad (2–3 km wide), lowland floodplain and including several settlements, notably the villages of Wellington, Marden and Moreton-on-Lugg. The course of the river meanders through the study area on a north–south orientation and is in parts characterized by a high degree of sinuosity (Dorling 2007, 55). In the central portion of the valley floor, gravel deposits are covered by up to 3 m of Holocene alluvium that had previously been variably described by British Geological Survey (BGS) mappers as being a homogeneous, fine clayey-silt deposit (Brandon 1989). However, (geo)archaeological research in the region has provided more detailed insights regarding the alluvial deposit sequence (Jackson and Miller 2011).

Numerous archaeological sites are known in the Lower Lugg valley, but many have only been discovered through phases of salvage excavations ahead of sand and gravel extraction. In particular, near the village of Wellington, investigations have exposed a range of significant and well-preserved multiperiod archaeological remains (Arnold and Jackson 2015, 2016; Carey et al. 2017; Jackson et al. 2013), including Neolithic, Beaker and Bronze Age ritual and funerary activity, Iron Age and Romano-British settlement remains, two substantial 8th-century AD structures including a timber water mill and extensive evidence for later mediaeval water management and cultivation practices (Jackson and Miller 2011). The archaeological remains from these time periods were variously located within and below differing amounts of alluvial sediment, with the most recent remains typically occurring in the near surface (<1 m) and earlier periods being much more deeply buried (+2 m). However, the distribution of these remains was also influenced

by subsurface (past) landforms and patterns of erosion and sedimentation. The higher, drier areas of the floodplain that were intersected by palaeochannels provided the focus for earlier prehistoric activity (e.g., funerary monuments and pit groups) and later prehistoric-Late Roman settlement and agriculture (Jackson and Miller 2011). Conversely, the lower lying wetter areas of the floodplain contained few archaeological remains, although palaeochannels provided rich palaeoenvironmental assemblages (Payne and Jordan 2011). These archaeological remains, landform assemblages and their associated environmental records provided a model for the changing landscape of the valley floor, as well as an important context for periods of occupation. Moreover, these investigations of this part of the floodplain have demonstrated that the Lower Lugg contained a chronologically diverse and exceptionally rich archaeological record that was intimately linked to the patterns and process of landscape evolution.

3.2 | Middle Wye Valley

The Middle Wye study area covers a 3.5×8.5 km area, extending between Hay-on-Wye and Letton, close to the Welsh-English border. Here, the floodplain measures between 1.5 and 2 km wide and is blanketed with Holocene alluvium, although there was limited information defining the depth of these sediments or the potential for archaeological remains; in contrast to the Lower Lugg valley, there had been limited archaeological investigations in the Middle Wye valley, and therefore, the understanding of the nature and extent of the archaeological resource is skewed towards more easily recognizable sites at the immediate periphery of the valley floor.

4 | Materials and Methods

4.1 | SAR Data

To investigate the Lower Lugg and Middle Wye valleys, 74 SAR images were acquired via the COSMO-SkyMed constellation archive (Agenzia Spaziale Italiana (ASI) 2015). COSMO-SkyMed is the largest constellation in orbit operating in the X-band, comprising four spacecraft, allowing short revisit times (Covello et al. 2010). The satellite system does not allow fully polarimetric observations (Biondi 2018) and the higher spatial resolution data collected in Stripmap (HIMAGE) mode only provides single-polarization images from the four polarization combinations available (in this case HH). Although the StripMap (PingPong) mode does provide dual-pol capability and opportunities to differentiate between backscattering responses in naturally vegetated areas and agricultural crops using alternating polarizations (i.e., HH/VV, HH/HV or VV/VH), these are only available for lower spatial resolution (15 m) and were therefore considered to be of limited use for geoarchaeological prospection (Tapete and Cigna 2019). Thus, only higher resolution Stripmap (HIMAGE) images were chosen for this analysis, spanning the period from 26 January 2014 to 31 March 2020, with an even temporal coverage over each year (approximately every 10 days), although there are fewer images available for 2014 and 2015. Each image was in HH polarization, with an incidence angle of 27° and a range and azimuth resolution of 5 m, providing a spatial resolution of 5 m for a 40 km² swath, spanning both the Lower Lugg and Middle Wye study areas (Figure 2b).

4.1.1 | Data Processing

COSMO-SkyMed SAR data can be delivered at a variety of processing levels, including a raw format comprising unpacked echo data in complex in-phase and quadrature signals (Level 0), single-look complex slant (Level 1A), ground multilooked (Level 1B), and geocoded ellipsoid (Level 1C) and terrain corrected (Level 1D). These steps reduce noise (multilooking), project the data or correct for geometric distortions. For this analysis, Level 1C data were selected, which provides data expressed as Digital Numbers (DNs), which were then converted to express attenuation in terms of decibels (dB) using a backscattering coefficient. This was calculated using the band math function in ENVI by the following formula:

$$\sigma^\circ = DN^2 \frac{1}{KF^2} \sin(\theta) R_{ref}^{2R_{exp}},$$

where σ° is the mean backscattering coefficient, θ is the reference incidence angle, R_{ref} is the reference slant range, R_{exp} is the reference slant range exponent, K is the calibration constant and F is the rescaling factor (after Baghdadi et al. 2015). This radiometric calibration makes each image more comparable and multitemporal analysis of the image series possible.

All SAR images are affected by a granular character commonly referred to as ‘Speckle’, which can complicate the identification of features. This is a consequence of coherent imaging (e.g., SAR systems transmit microwave pulses that are phase coherent), and although it should not be considered ‘noise’, it can be detrimental

to the quality of the image. One approach to overcome this speckling is adaptive filtering, but as the visibility of archaeological and geomorphological features can be subtle, a compromise is needed to enable satisfactory filtering of the speckle effect whilst also ensuring that features of interest remain (Lasaponara et al. 2017). In most cases, it is necessary to consider different approaches to speckle filtering (e.g., Chen et al. 2015). Following trialling of numerous filtering procedures on the studied data using ENVI (NV5 Geospatial), it was found that a Lee filter with a moving window of 3×3 (pixels) provided the best image clarity and feature visibility and was therefore used in each image, similar to Gade, Kohlus, and Kost (2017). This process did not filter out all the speckle but using larger windows (> 3 m) resulted in a loss of feature definition and the moving window of $5 \text{ m} \times 5 \text{ m}$ was selected as the best compromise between improved data quality whilst allowing alluvial landforms to be visualized.

4.2 | Auger Transects

To complement and validate any visible surface features identifiable in the SAR data, a series of gouge core (auger) transects were also collected to elucidate the subsurface stratigraphy. Deposit models typically integrate at least some information from intrusive investigations to provide an understanding of subsurface sediment architectures, for deeply alluviated sequences, this is normally achieved through a series of auger samples or boreholes across an area of interest in a targeted or gridded manner, either undertaken with a hand auger or machine-drilling rig (Carey et al. 2018). For this investigation, a series of hand-driven gouge core auger transects were positioned perpendicular to the floodplain corridor to provide two-dimensional, vertical cross-sections of stratigraphic units across each study area.

The gouge auger had a 2-cm barrel, and each auger sample was spaced between 50 and 150 m apart, allowing the depths and visible changes in sediment composition to be logged through visual observation and qualitative description (Canti et al. 2015). Although a more consistent spacing between augering was desirable, the larger gaps of up to 150 m only occur in a small number of cases due to land access issues (e.g., inaccessible areas or where landowner permission was denied). The data from the auger samples were added to a database together with a GPS location and combined with elevation data derived from available lidar. These data were then imported into Strater 5, a borehole and cross-section plotting software package (Golden Software), enabling multiple gouge-core transects (or cross-sections) to be produced of the sediment sequence in each case study area.

5 | Maximizing the Visibility of Alluvial Landforms in SAR Data

Individual SAR backscatter images are typically displayed using a linear grey scale, with black representing low intensity and white high intensity (Tapete and Cigna 2019). Although these individual images are valuable for distinguishing types of land cover, further information can be contained within a time series of images, but due to their high data dimensionality, this can be difficult to interpret. This is pertinent to the high temporal resolution of COSMO-SkyMed time

series, and various methods can be used to prevent data redundancy. Conventionally, this is targeted towards change detection approaches aimed at documenting impacts caused by environmental processes or anthropogenic activities (Cigna et al. 2023). However, this investigation was not concerned with change; rather, it focussed on understanding persistent/consistent anomalies. Consequently, change detection approaches are not applicable, and other solutions were sought, primarily including composite images, the calculation of basic metrics (e.g., minimum, mean and maximum values) and dimensionality reduction (principal component analysis [PCA]). As there have been no previous attempts to summarize SAR data time series in this manner, it was necessary to evaluate these approaches to establish an optimal methodology for geoarchaeological investigations. This was focussed on part of the Lower Lugg valley case study area, where known alluvial landforms were previously recorded (Crabb et al. 2022), to establish which approach was most effective, which could then be applied more widely in the Lower Lugg and across the Middle Wye valleys.

5.1 | Evaluation of SAR Data

Although separability measures can be used to evaluate the capability of lidar visualization and multispectral image enhancement techniques (e.g., Crabb et al. 2022, 2023), these are difficult to apply to a time series of SAR data. This is due to the complexity surrounding the interpretation of backscatter intensity data collected on multiple different dates, as land use and ground conditions vary significantly across the year. As noted previously, most SAR imagery is also characterized by inherent noise or speckle, making it difficult to quantify the effectiveness of an image based on the histograms of regions of interest. Thus, a visual comparison of the transformed images produced from the COSMO-SkyMed data was undertaken.

5.1.1 | Individual Radar Images

It is not practical here to present all 74 images of the COSMO-SkyMed time series but an illustration of the temporal character of the data (from March 2019 to March 2020) is provided in the [Supporting Information](#), which highlights some salient characteristics of the radar backscatter features observable in the data.

In most temperate (rural) floodplain settings, the prevailing surface response recorded in radar imagery is attributable to vegetation, which forms a complex, heterogeneous volume of material comprising both the vegetation structure and underlying soil. There is variation amongst according to different land use surface characteristics such as grass or type of arable crop. Within an individual land parcel or field of land use, further variation can be observed that potentially relate to subsurface changes, but these are difficult to define, as the response of the SAR produces a very 'speckled' appearance. Within bare soil fields, there was more limited variation relating to alluvial landforms due to the prominent levels of noise caused by increased surface roughness associated with ploughed soil surfaces. More positively, areas of surface flooding recorded during winter months

delineated several clear palaeochannels and showed places that consistently flood, even during periods of more limited rainfall (e.g., Figure 3a–f). As the definition of such landforms within floodplains is central to the construction of deposit models, this provided the focus for the application of the SAR imagery.

5.1.2 | Composite Radar Images

Composite imagery for SAR datasets commonly consists of different image polarizations (e.g., HH, HV and VV) to visualize different forms of backscatter anomalies (Lasaponara and Masini 2013). As COSMO-SkyMed data collected in Stripmap (HIMAGE) mode only provide single-polarization images (in this case HH), this was not possible. However, the combination of multiple images from a time series in a composite can help to summarize data collected from a maximum of three dates. When considering the extent of flooding, three images were selected to cover the episode including the outset, peak and dissipation of flood water. An example of such a composite image is shown in Figure 3g,h, which details the flooding in early 2014 (R=26/01/2014, G=11/02/2014 and B=16/06/2014). These represent the only images available for this period of flooding and, which clearly define palaeochannels and areas that consistently flood, which can be used as a proxy for identifying such landforms. However, they are only derived from three images (dates), and it is possible that other, more subtle, backscatter anomalies may be present in the time series.

5.1.3 | Summarizing the Time Series

Interpreting multiple images from a time series is labour intensive, and, as information is often repeated across images from different dates, it is useful to reduce this high data dimensionality. One approach used to achieve this was to calculate the minimum, mean and maximum backscatter values so that persistent backscatter anomalies might be more apparent. Each of these metrics was calculated using the cell statistics function in ArcGIS to produce raster images and combined to create a composite image combining all three variables (see Figure S3). In these images, the minimum backscatter intensities were associated with flooding and bare soil, whereas maximum backscatter was attributable to low canopy vegetation (crops), hedgerows and buildings. Because there is a significant difference between the specular response of flooding and the more complex response of vegetation (during drier parts of the year), the mean backscatter image showed limited variation, as the higher backscatter responses were counteracted by the low (specular) response of floodwater. In attempt to overcome this, the time series was partitioned into flooded (i.e., floodwater was visible in the SAR image as a specular response), and nonflooded subsets and the same metrics were calculated (see Figures S4 and S5). The flooded data (comprising 23 images) were effective at defining landforms but were less clear than the simple combination of images as a composite and were therefore not deemed appropriate for this analysis.

Another approach to summarizing the SAR time series adopted was PCA. This is widely used in remote sensing and operates by identifying interband correlations (in this case, images collected

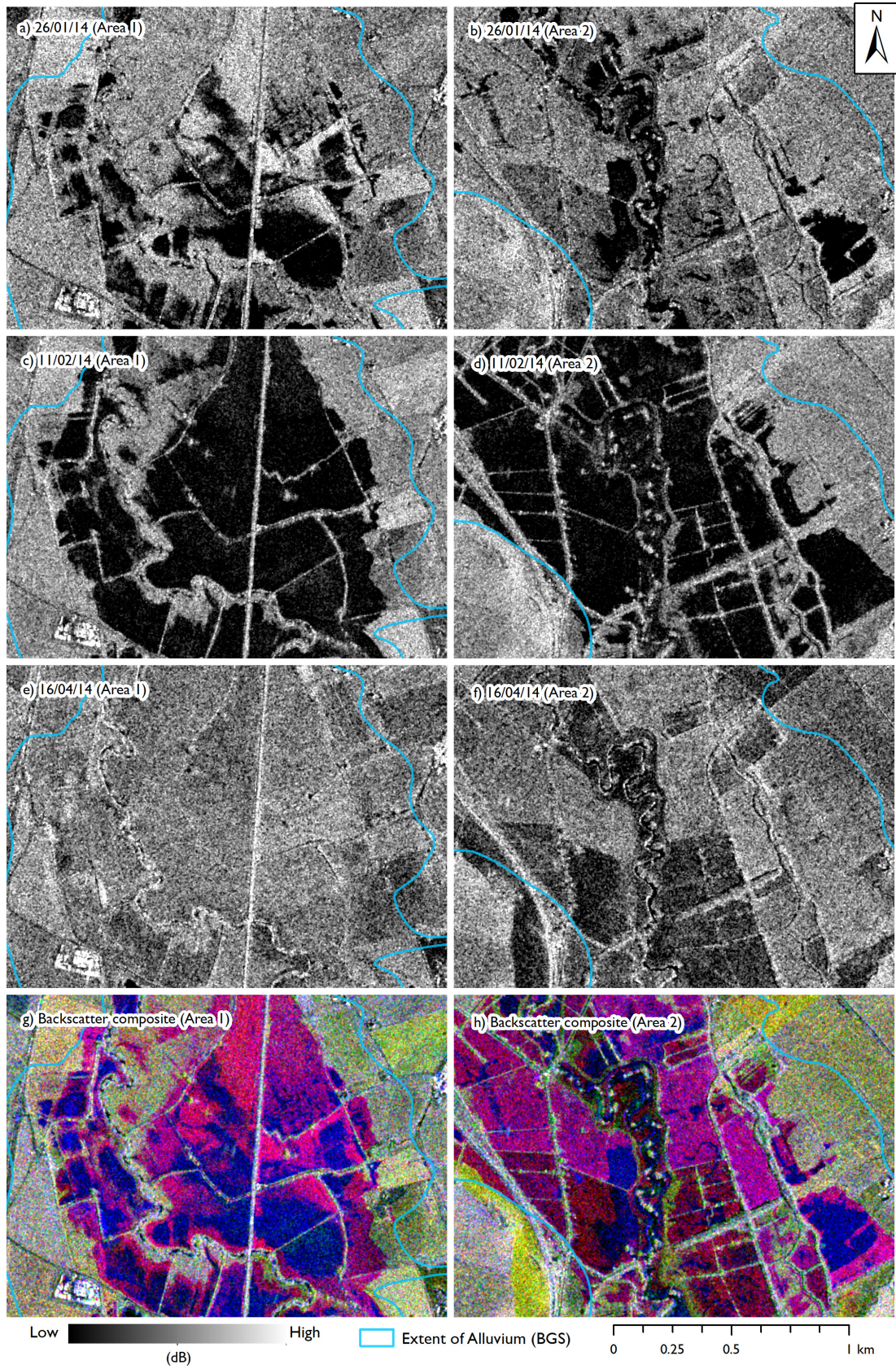


FIGURE 3 | Individual SAR images and RGB composite images two image comparison areas from the Lower Lugg valley, illustrating flooding from the winter of 2014.

on different dates) and transforming the data into new (component) bands (Lasaponara and Masini 2012, 37). The result is that most of the variance in the resulting dataset is summarized by the first component, with subsequent components containing a lower proportion of the dataset variance. For this research, PCA was calculated using covariance matrices in ENVI for the entire time series, as well as the subsets of 23 images that contained flooding and the 51 without. Because the major proportion of the variance is contained within the first three components, the results can be presented together as a composite image comprising these new component bands (e.g., R = PC1, G = PC2 and B = PC3). It was hoped that this would enable ore subtle alluvial landforms to be visualized, but the PCA composite tended to only summarize similar land use characteristics across the time series such as lower backscatter intensity regions associated with lower lying, flooded regions (see Figure S6). In addition, as encountered previously, the definition of landforms within these images was generally poor due to inherent diversity caused by the specular response of flood water. Although results were marginally improved when the PCA was restricted to the flooded and nonflooded subsets of the time series, this did not match the level of clarity provided by a the more simple composite derived from individual images covering a single flood episode such as that shown in Figure 3.

5.1.4 | Implications for Understanding Subsurface Complexity

Although limited to three images from the COSMO-SkyMed time series, composite images covering a flood episode from 2014 provided the strongest definition of landforms (Figure 3g,h). This effectively uses the extent of flooding as a proxy for subtle surface topographic variations but also highlights areas that persistently flood independent of topography, which are influenced by the presence of subsurface landforms such as any palaeochannels or lower lying topographic zones that are not expressed topographically. Although this is an unconventional approach to the visualization of data derived from a SAR time series, it correlates very well with the definition of landforms provided by lidar in previous geoarchaeological investigations (Carey et al. 2018; Crabb et al. 2023). Thus, these 'flood composites' were selected for the construction of deposit models of the Lower Lugg and Middle Wye valleys.

6 | Results

A detailed geoarchaeological interpretation of the SAR flood composites was undertaken for both the Lower Lugg and Middle Wye valleys. This was achieved by digitizing features as polygons (.shp files) in ArcGIS relating to a consistent set of interpretation categories, including

- Palaeochannels: sinuous/linear depressions, filled with surface water during flooding.
- Higher topographic zone: areas that remain dry during flooding episodes.
- Lower topographic zone: areas covered by surface water during periods of flooding.

The interpretation of the SAR data was then compared against the vertical profiles generated from auger core transects (a summary of the salient details of the sediment units detailed in these cross-sections and their probable depositional context is provided in Tables S2 and S3). For ease of reference, each study area has been divided into three subsections described in detail below: Areas LLa–LLc and MWa–MWc. Each feature is described in Tables 1 and 2, together with an indication of its archaeological potential and palaeoenvironmental preservation capacity, but a more detailed discussion of the salient landforms is provided for each area below.

6.1 | Lower Lugg Valley

The flood composite for the Lower Lugg valley defined numerous palaeochannels within a number of topographic zones. This facilitated the production of a geoarchaeological deposit model (Figure 4), together with cross-sections produced from the auger samples (Figure 5) and detailed SAR images (Figures 6–8).

6.1.1 | Area LLa

In the northern part of the Lower Lugg valley (Area LLa), a network of sinuous palaeochannels was visible that were infilled with silt and organic-rich deposits (Transect LLa; Figure 4). These are most clear along the eastern edge of the floodplain corridor, adjacent to a modern drainage ditch (LL1), becoming wider towards the auger transect in the southwest (LL2; Figure 6). This arrangement of multiple channels and channel fragments potentially represents the remnants of an early (later Pleistocene/Early Holocene) multichannel braidplain. This probably developed into an avulsive channel system in the later Holocene, consistent with evidence from Wellington Quarry, indicating the river rationalized into fewer channels following the end of glacial conditions as the climate ameliorated into the early Holocene (Mesolithic) and as discharge was reduced (Payne and Jordan 2011).

Further evidence for paleochannels in the northern part of the Lower Lugg valley was identified west of Burling Gate Farm (LL3), but it was difficult to determine the lateral (spatial) extent of these features due to the presence of modern boundary and drainage features. Despite this, it is likely that they continue further south, possibly as far as Manor farm (LL4). Broader palaeochannels were also visible on the western edge of the floodplain, but these were poorly defined within a broader lower topographic zone (LL5). These low-lying nature of these palaeochannels and the associated high-water table suggest a high potential for organic preservation and hence palaeoenvironmental reconstruction.

Along the western edge of the floodplain was an extensive area where the floodwater did not reach during the most extensive flood events (LL7). This corresponds with the location of previously recorded cropmarks identifying a probable Bronze Age enclosure (Herefordshire Archaeology 2015). Therefore, this area of floodplain edge has a high archaeological potential, a product of the higher topography of a Pleistocene terrace remnant, as indicated in the western part of Transect LLa, where more

TABLE 1 | Summary of alluvial landforms identified in the Lower Lugg valley indicating their archaeological potential and palaeoenvironmental preservation capacity.

	Feature number	Feature type	Description	Archaeological potential	Paleoenvironmental preservation capacity
LLa	LL1	Palaeochannel	Sinuuous palaeochannels adjacent to modern drainage ditch	Low	High
	LL2	Palaeochannel	Southern continuation of sinuous palaeochannels, but becoming wider towards Transect LLa.	Low	High
	LL3	Palaeochannel	Further sinuous palaeochannels on the eastern edge of the floodplain corresponding with deposits in Transect LLa.	Low	High
	LL4	Palaeochannel	Channel fragments adjacent to highly sinuous section the River Lugg.	Low	High
	LL5	Palaeochannel	Broad palaeochannels on the western edge of the floodplain, which are poorly defined, most likely due to the extent of flooding occupying adjacent low-lying areas.	Low	High
	LL6	Lower topographic zone	Area of very low-lying topography on the northwestern edge of the valley. There are no clear palaeochannels, but the area floods regularly.	Low	Moderate
	LL7	Higher topographic zone	Extensive area on the western edge of the floodplain, where the floodwater did not reach during the most extensive flood events.	High	Low
	LL8	Higher topographic zone	Narrow high point that is only covered by surface water when the flood is at its maximum (LL8) that corresponds with thinner units of alluvial sediment in Transect LLa.	High	Low
LLb	LL9	Palaeochannels	One broad and one narrow palaeochannel, defining higher topographic zones on either side.	Low	High
	LL10	Lower topographic zone	Large area consistently covered by surface water associated with a lower lying back-basin of the floodplain with a deeper alluvial sequence and higher water table.	Low	Moderate
	LL11	Lower topographic zone	Fields inundated through the period of flooding in 2014 on the eastern side of the River Lugg.	Low	Moderate
	LL12	Palaeochannels	Poorly defined lower lying landforms, which are closely related to the earthworks of the moat, fishponds and other features pertaining to the early mediaeval magnate's residence at Freen's Court.	Low	High
	LL13	Palaeochannels	Sinuuous depressions that regularly flood south of the present course of the River Lugg. These correspond with palaeochannel deposits in the southwest of Transect LLb, where grey silt-rich deposits containing abundant organic material were identified.	Low	High
	LL14	Modern woodland	Area of woodland where high backscatter intensity is recorded, which is consistent with vegetation that is underlain by surface water.	Unknown	Unknown

(Continues)

TABLE 1 | (Continued)

	Feature number	Feature type	Description	Archaeological potential	Paleoenvironmental preservation capacity
LLc	LL15	Palaeochannel	Narrow palaeochannel which regularly floods. Although not clear in the SAR data, this continues towards the southeast, as demonstrated by the presence of palaeochannel deposits in Transect LLc, suggesting it continues along the western edge of the floodplain corridor.	Low	High
	LL16	Higher topographic zone	Area covered by surface water when flooding is at its peak, but otherwise remains dry. The area occupies a slight rise in the landscape, where the depth of alluvium is shallow in Transect LLc.	High	Low
	LL17	Palaeochannels	East of the contemporary channel of the River Lugg, at least one highly sinuous meandering palaeochannel was visible. This follows the same orientation as the present river and closely relates to a series of organic-rich palaeochannel deposits identified in Transect LLc.	Low	High
	LL18	Palaeochannels	The palaeochannel at LL17 continues south throughout the remainder of Area LLc.	Low	High
	LL19	Palaeochannels	Adjacent to the course of a minor stream called 'The Rhea', there are a small number of discrete depressions that relate to further palaeochannels.	Low	High
	LL20	Lower topographic zone	Elements of a narrow feature associated with the confluence of the Lugg and a minor tributary are apparent as a regularly flooding, lower topographic zone.	Low	Moderate
	LL21	Lower topographic zone	A lower lying, frequently flooded area, which corresponds with the remains of a postmediaeval water meadow system	Low	Moderate

freely draining sands and gravels, attractive for past human settlement, are present. Close to Green Farm, there is also a narrow high point that is only covered by surface water when the flood is at its maximum (**LL8**) that corresponds with thinner units of alluvial sediment in Transect LLa (Figure 4). This represents a higher topographic zone associated with a narrow gravel ridge or natural levee, providing another area of high archaeological potential, on a drier upstanding landform.

6.1.2 | Area LLb

The north-western part of Area LLb covers the environs of Wellington Quarry and its recently excavated (post-2014) southern extension, with many landforms visible in the SAR flood composite imagery predating the extraction (Figure 7). This included one broad and one narrow palaeochannel, which defines higher topographic zones on either side (**LL9**). These landforms correlate very well with a previous smaller scale deposit model produced from lidar data in this area (Carey et al. 2017), the predictions of which have been confirmed through subsequent archaeological monitoring of the site.

In the north of Area LLb, east of Wellington Quarry, there is a large area consistently covered by surface water (**LL10**). This is

associated with a lower lying back basin of the floodplain where a deeper alluvial sequence and higher water table is expected, thereby enhancing the potential for paleoenvironmental preservation. Directly east, within the northernmost part of Wellington Quarry, a series of highly irregular shaped shallow pools and backswamps were identified (Jackson and Miller 2011), and it is possible that similar channel-like deposits to those identified in the excavation areas are located within **LL10**.

On the eastern side of the River Lugg, to the south of Marden, the fields were inundated through the period of flooding in 2014, indicating another topographically lower area (**LL11**). Further evidence for lower topographic zones has also been recorded to the south of this (**LL12**), but they are poorly defined in the SAR data, as their lower topographic position is closely related to the earthworks of the moat, fishponds and other features pertaining to the early mediaeval magnate's residence at Freens Court (Historic England 2024a).

Close to the present course of the River Lugg, there are short but sinuous depressions that regularly flood, which likely pertain to palaeochannels (**LL13**). These correspond with palaeochannel deposits in the southwest of Transect LLb, where grey silt-rich deposits containing abundant organic material were identified (Figure 4).

TABLE 2 | Summary of alluvial landforms identified in the Middle Wye valley indicating their archaeological potential and palaeoenvironmental preservation capacity.

Area	Feature number	Feature type	Description	Archaeological potential	Paleoenvironmental preservation capacity
MWa	MW1	Palaeochannel	An isolated area of flooding on the western side of the River Wye In the east of Area MWa.	Low	High
	MW2	Palaeochannels	Several palaeochannels identifiable as flooded areas in the centre of the floodplain. These landforms correspond very well with organic-rich deposits in auger Transect MWa.	Low	High
	MW3	Palaeochannels	Several palaeochannels identifiable as flooded areas in the centre of the floodplain. These landforms correspond very well with organic-rich deposits in auger Transect MWa.	Low	High
	MW4	Palaeochannels	Numerous palaeochannels beyond the mapped extent of the valley floor corridor at Sheepcote Farm.	Low	High
	MW5	Lower topographic zone	Areas of high backscatter intensity indicative of saturated ground producing a yellow-speckled texture and indicating lower lying (wetter) subsurface topographic zones	Low	Moderate
MWbye	MW6	Palaeochannels	Network of palaeochannels, the definition of which is poor, although Transect MLb revealed at least 5 possible palaeochannels.	Low	High
	MW7	Palaeochannels	Evidence for ridge and swale landforms relating to the lateral migration of the river.	Low	High
	MW8	Palaeochannels	Narrow palaeochannels close to the edge of the floodplain, which run parallel to the present course of the river.	Low	High
	MW9	Palaeochannels	Possible meander loop extending from MW9.	Low	High
	MW10	Palaeochannels	Numerous palaeochannel fragments on southern side of River Wye	Low	High
	MW11	Palaeochannel	Broad palaeochannel heading south on the northern limit of the floodplain, adjacent to a small stream.	Low	High
	MW12	Palaeochannel	Sinuuous palaeochannels, south of the village of Stow, which regularly flood.	Low	High
	MW13	Palaeochannels	Subcircular depressions that flood regularly. These are likely associated with low-lying and 'hummocky' deposits	Low	High

(Continues)

TABLE 2 | (Continued)

Area	Feature number	Feature type	Description	Archaeological potential	Paleoenvironmental preservation capacity
MWc	MW14	Palaeochannels	Ridge and swale are evident adjacent to an acute bend in the present course of the Wye	Low	Moderate
	MW15	Palaeochannel	Broad palaeochannel located in the centre of the floodplain.	Low	High
	MW16	Palaeochannel	Possible continuation of MW16 south of Rockville House	Low	High
	MW17	Palaeochannel	Several cutoff meanders located east of the Holm.	Low	High
	MW18	Palaeochannel	Palaeochannel that turns south towards Clock Mills but has been truncated by the present course of the Wye.	Low	High
	MW19	Palaeochannel	A series of more discrete palaeochannels south of Court Farm.	Low	High

6.1.3 | Area LLc

A large proportion of Area LLc is consistently covered by floodwater (Figure 8). This compares extremely well with the thicker sequences of the floodplain recorded along Transect LLc (Figure 4). The eastern part of the valley, around Sutton Marsh, is less extensively covered by surface water, indicating a slightly higher area where floodwaters rarely reach. In contrast, on the western side of the floodplain, a narrow palaeochannel is visible (LL15), which correlates with palaeochannel deposits in Transect LLc.

In an area where the Neolithic standing stone known as the ‘Wergins’ Stone is located (Historic England 2024b), the area is only covered by surface water when flooding is particularly severe and at its peak (LL16). Although the surface topography is not sufficient to prevent the area from being flooded, the standing stone does occupy a dryer part of the floodplain. This absence of regular flood inundation is also reflected by the shallow depth of alluvium in Transect LLc (Figure 4).

East of the contemporary channel of the River Lugg, at least one highly sinuous meandering palaeochannel was visible (LL17). This follows the same orientation as the present river and closely relates to a series of organic-rich palaeochannel deposits identified in Transect LLc (Figure 4). The palaeochannel is positioned in a lower topographic zone that frequently floods and continues south throughout the remainder of Area LLc towards Eau Withington (LL18).

In the east of Area LLc, adjacent to the course of a minor stream called ‘The Rhea’, there are a small number of discrete depressions that relate to further palaeochannels (LL19). These are located close to the edge of the floodplain but were not identified in Transect LLc, as the auger cores missed these features. Further east, elements of a narrow feature associated with the

confluence of the Lugg and a minor tributary are also apparent as a regularly flooding, lower topographic zone (LL20).

In the south of Area LLc, west of Shelwick Green, there is a lower lying, frequently flooded area, which corresponds with the remains of a postmediaeval water meadow system (LL21). This (historic) land management practice increases the retainment of surface water but indicates a further lower lying area, which may have a higher potential to preserve palaeoenvironmental remains.

6.2 | Middle Wye Valley

The SAR flood composite for the Middle Wye valley delineated a series of palaeochannels and a small number of lower topographic zones. The deposit model produced from these interpretations is presented in Figure 9 with the auger core transects (Figure 10) and SAR images shown in Figures 11–13. These zones are less extensive than those identified in the Lower Lugg valley, but the flood composites define the lowest lying and wetter elements of palaeochannels, where anoxic conditions are more prevalent. However, the imagery does not identify any clear, higher topographic zones where settlement activity might have been preferentially focused.

6.2.1 | Area MWa

In the east of Area MWa, northeast of Clifford, there is an isolated area of flooding on the western side of the River Wye (MW1; Figure 11). This is associated with a palaeochannel, but is only partially visible, most likely relating to the lowest lying aspects of the feature. However, several paleochannels are identifiable as flooded areas in the centre of the floodplain (Figure 11; MW2 and MW3). Although these are notably less extensive than was apparent for

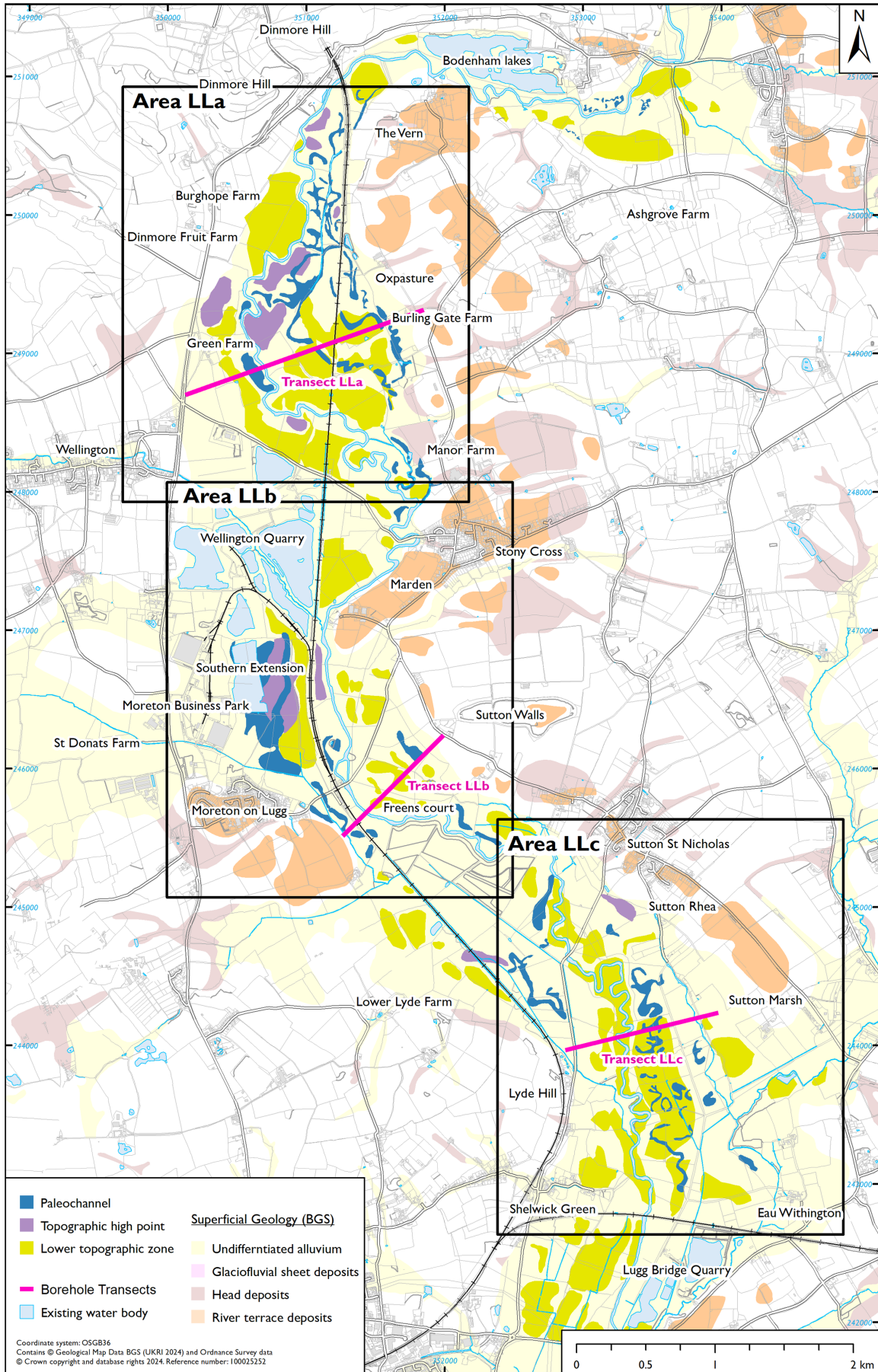


FIGURE 4 | Geoarchaeological deposit model of the Lower Lugg Valley produced from the interpretation of SAR data.

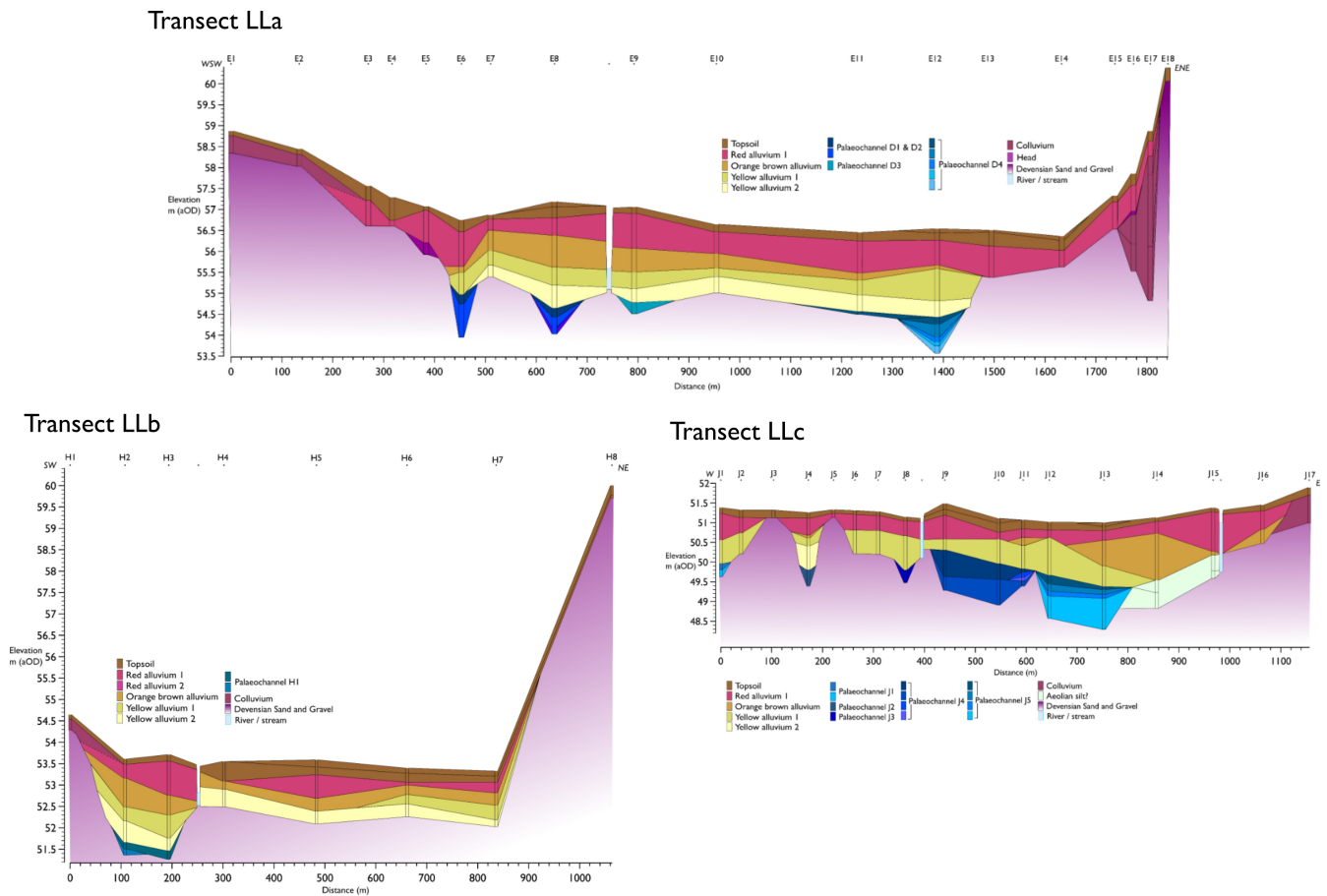


FIGURE 5 | Borehole Transects LLa, LLb and LLc (south facing) displayed at the same vertical and horizontal scale, with a consistent colour scheme pertaining to the observed sediment units.

the Lower Lugg valley, these landforms correspond very well with organic-rich deposits in auger Transect MWa (Figure 10).

Surrounding Sheepcote Farm in the east of Area MWa, there are numerous palaeochannels beyond the mapped extent of the valley floor corridor (MW4). This indicates that the southern part of the floodplain is more extensive than is recorded by geological mapping of alluvium, which is corroborated by deposits recorded in Transect MWa, which includes a considerable proportion of coarser grained sands indicative of higher energy pulses of sedimentation. Some fields near Sheepcote Farm are also visible as areas of high backscatter intensity, which is indicative of saturated ground, producing a yellow-speckled texture and indicating lower lying (wetter) subsurface topographic zones (MW5). These areas were characterized by a high degree of soil moisture throughout the winter of 2014 but became drier in the spring.

6.2.2 | Area MWb

The flood composite for area MWb defined palaeochannels, but some aspects of these are poorly represented (Figure 12). For example, around Transect MWb, individual channels cannot easily be recognized, as the entire area is inundated by floodwater, apart from a small number of high points (MW6). Transect

MLb, however, did identify at least five possible palaeochannels infilled with fine and coarse-grained sandy sediments (Figure 9).

Close to a large bend in the river to the south of Whitney-on-Wye, there was extensive flooding close to the present channel, within which narrow higher and drier zones are apparent (MW7). These are associated with ridge and swale landforms relating to the lateral migration of the river that can result in the reworking of floodplain sediments. Such landforms are rarely conducive to the preservation of in situ archaeological and paleoenvironmental material. Yet, despite being of lower value than in situ remains, the position of reworked archaeological remains, ridge and swale can provide important information with respect to floodplain evolution as exemplified by studies in the Middle Trent (Salisbury 1984, 1992).

North of the River Wye, west of Stowe Pool, several narrow palaeochannels are visible close to the edge of the floodplain (MW8), which run parallel to the present course of the river and form a large meander loop east of Area MWb (MW9). Further palaeochannels are apparent south of the River Wye near Lower Castleton Farm (MW10) and adjacent to a small stream southwest of Stowe (MW11). The latter may represent another former course of the Wye albeit following an alternative trajectory from Whitney-on-Wye.

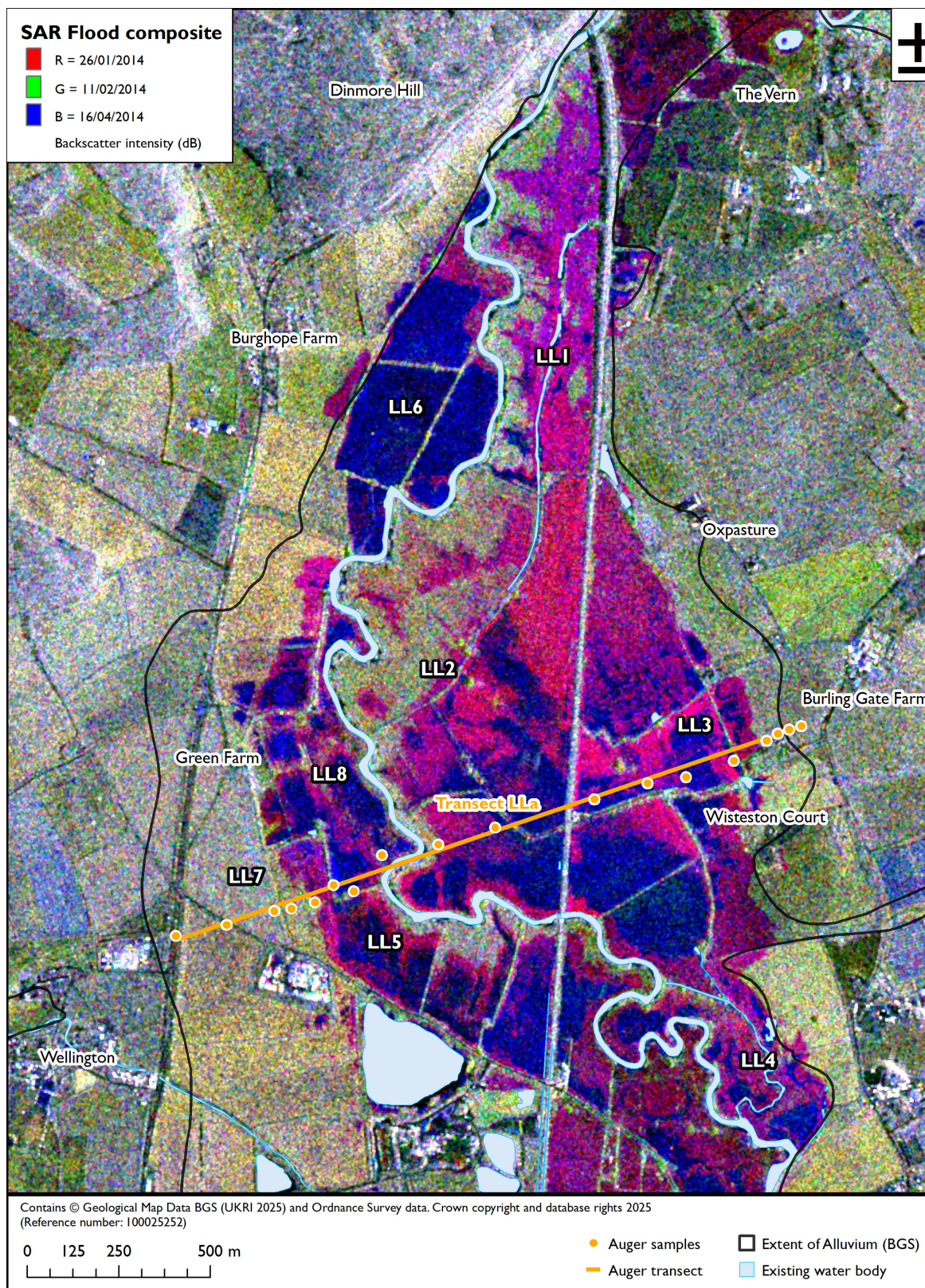


FIGURE 6 | SAR flood composite (Winter 2014) for Area LLa.

To the southeast of Stowe, there are more sinuous palaeochannels, which were frequently flooded and low lying (MW12). These may relate to early phases of the river system, potentially defining part of a relic braided pattern that later coalesced into

larger channels. Although no clear higher topographic zones have been identified by the SAR data in this area, the dry zones adjacent to these channels have potential to preserve archaeological remains.

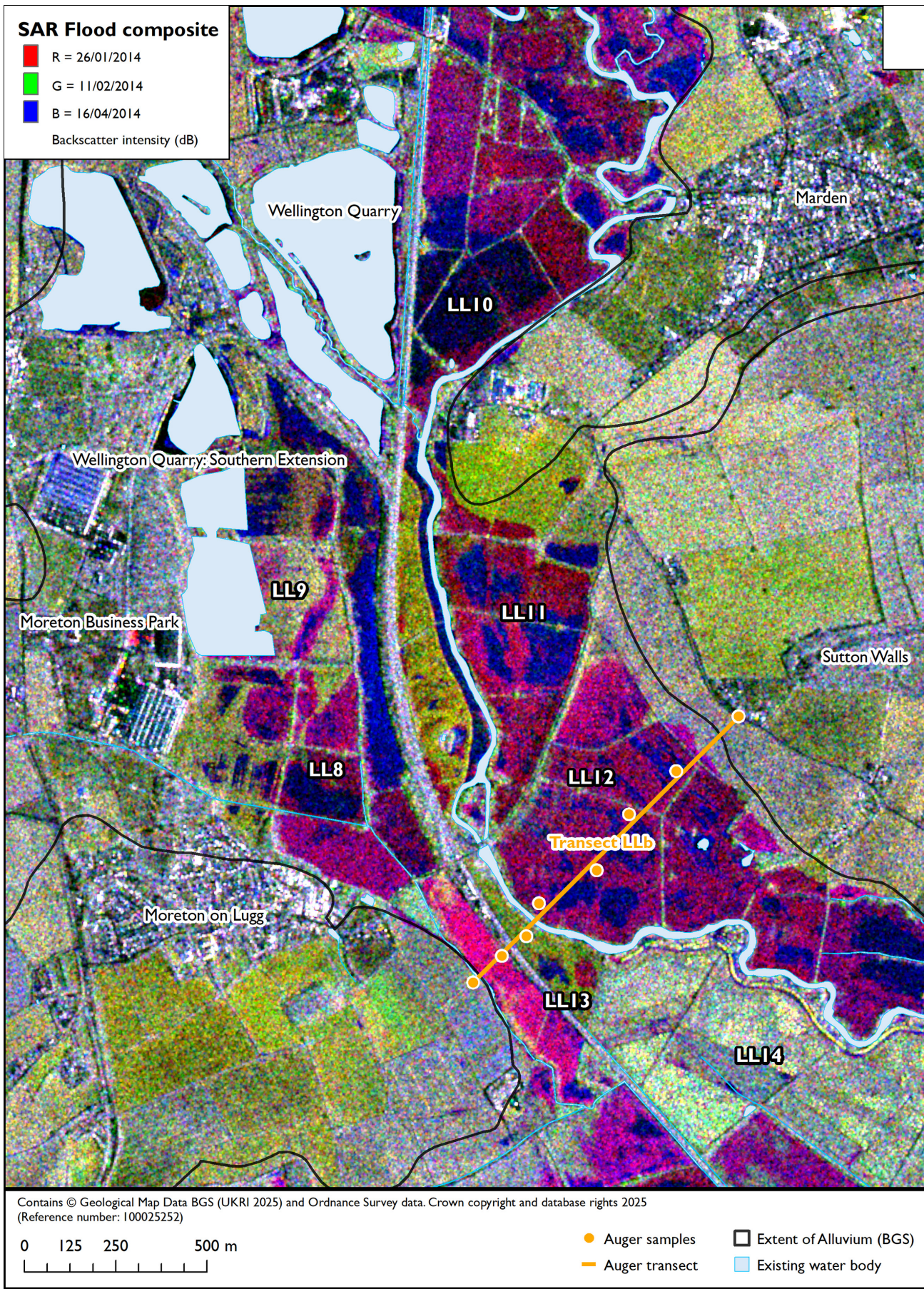


FIGURE 7 | SAR flood composite (Winter 2014) for Area LLb.

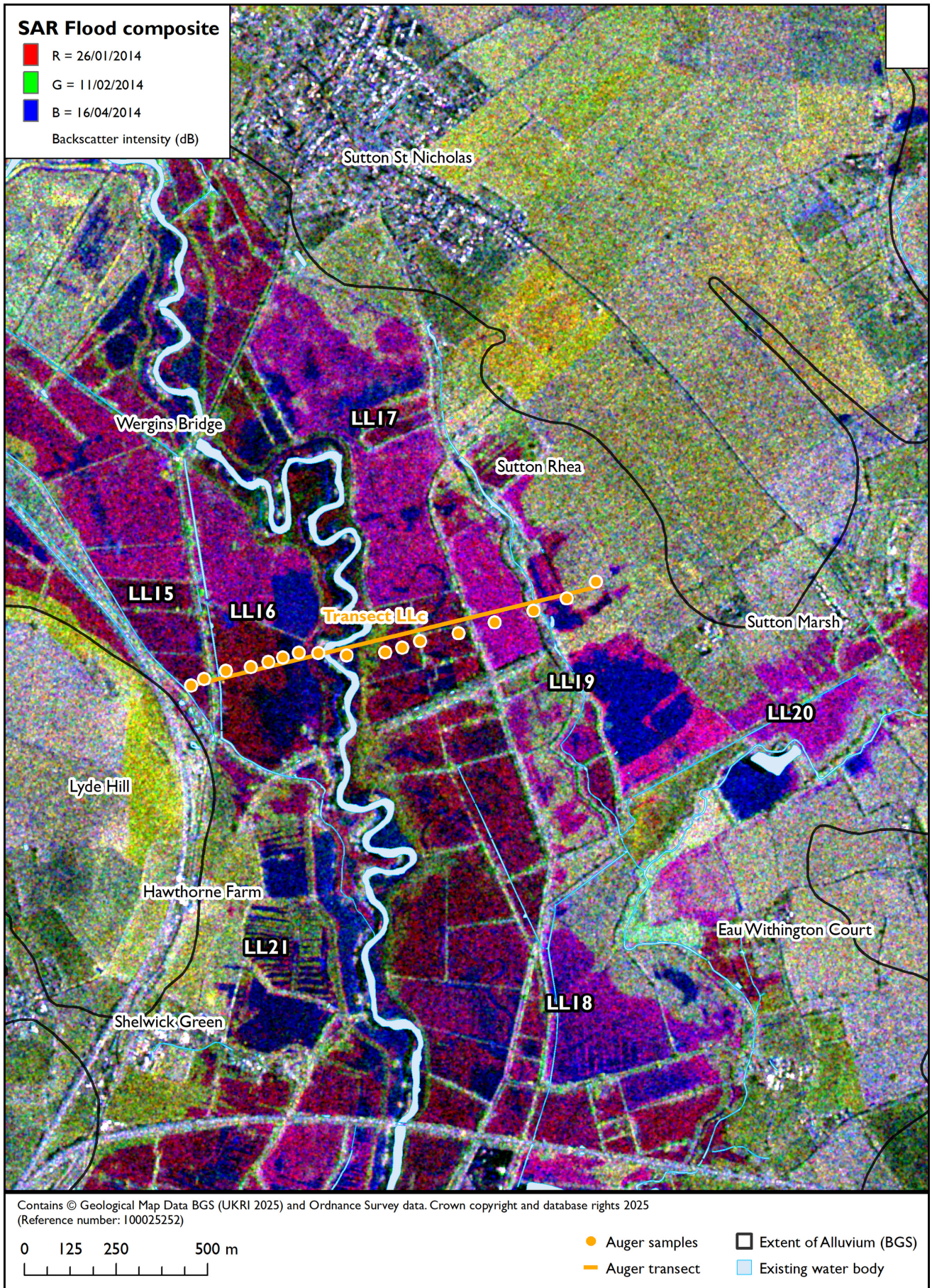


FIGURE 8 | SAR flood composite (Winter 2014) for Area LLc.

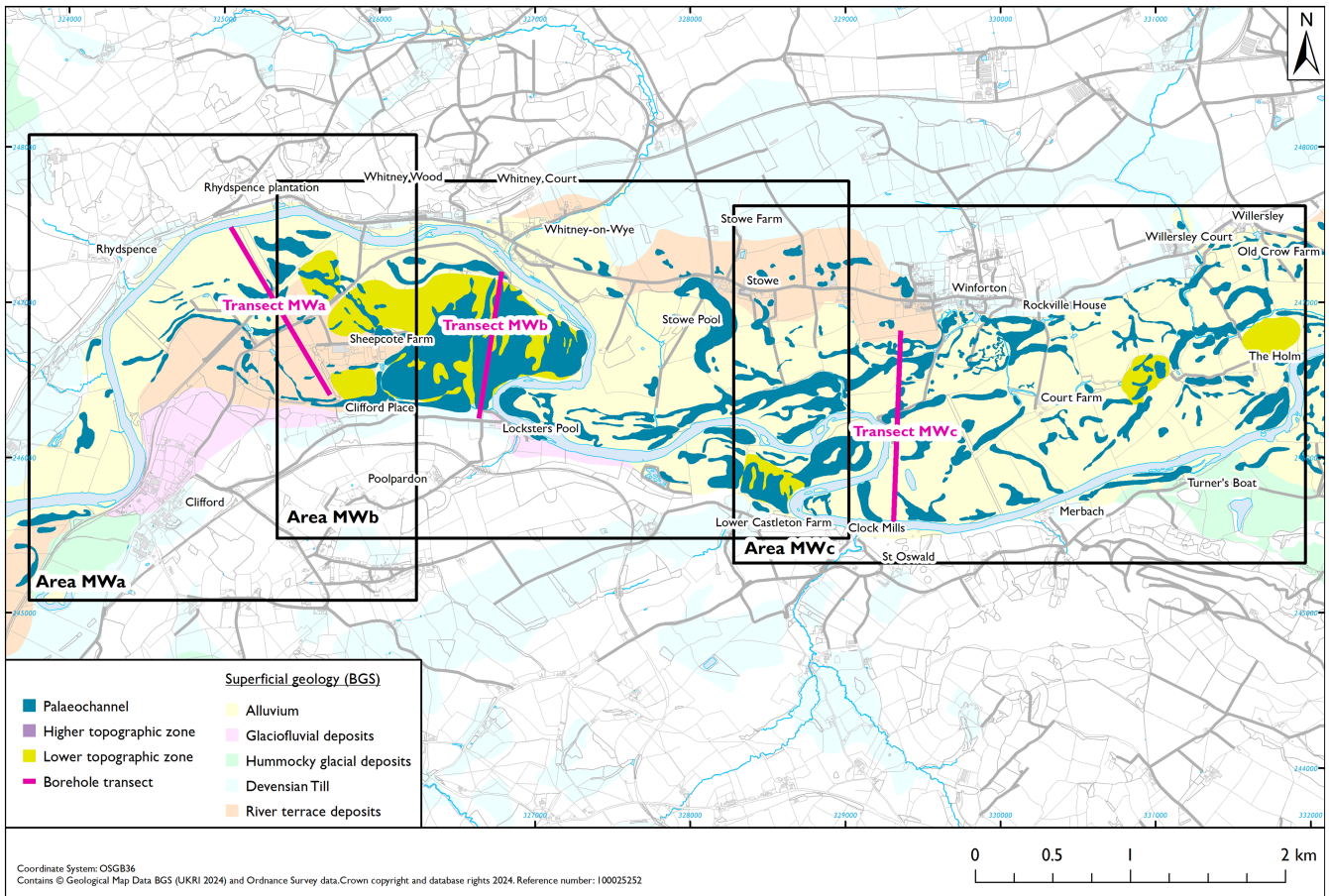


FIGURE 9 | Geoarchaeological deposit model of the Middle Wye Valley produced from the interpretation of SAR data.

Beyond the floodplain and north of the village of Stowe (**MW13**), there are numerous subcircular depressions that flood regularly. These are likely associated with low-lying and ‘hummocky’ deposits associated with a past glaciolacustrine environment, which have been previously mapped north and west of the Middle Wye Valley (Gurney, Astin, and Griffiths 2010). These topographic low points would have been clearly recognizable within the early Holocene landscape and may therefore have been foci for early postglacial archaeological activity.

6.2.3 | Area MWc

In the southwest of Area MWc, ridge and swale are evident adjacent to an acute bend in the present course of the Wye (**MW14**; Figure 13). To the north of the river, numerous palaeochannels are visible (**MW15**), and there are cutoff meanders in the centre of Area MWa at **MW16** and close to the Holm (**MW17**) in the west of the area.

Heading west from Court Farm in the centre of the floodplain is a palaeochannel that turns southwards towards Clock Mills but has been truncated by the present course of the Wye (**MW18**). North of this, there are numerous other channels that likely correspond to former courses of the river, though they are not recorded in Transect MWc as the auger cores narrowly missed

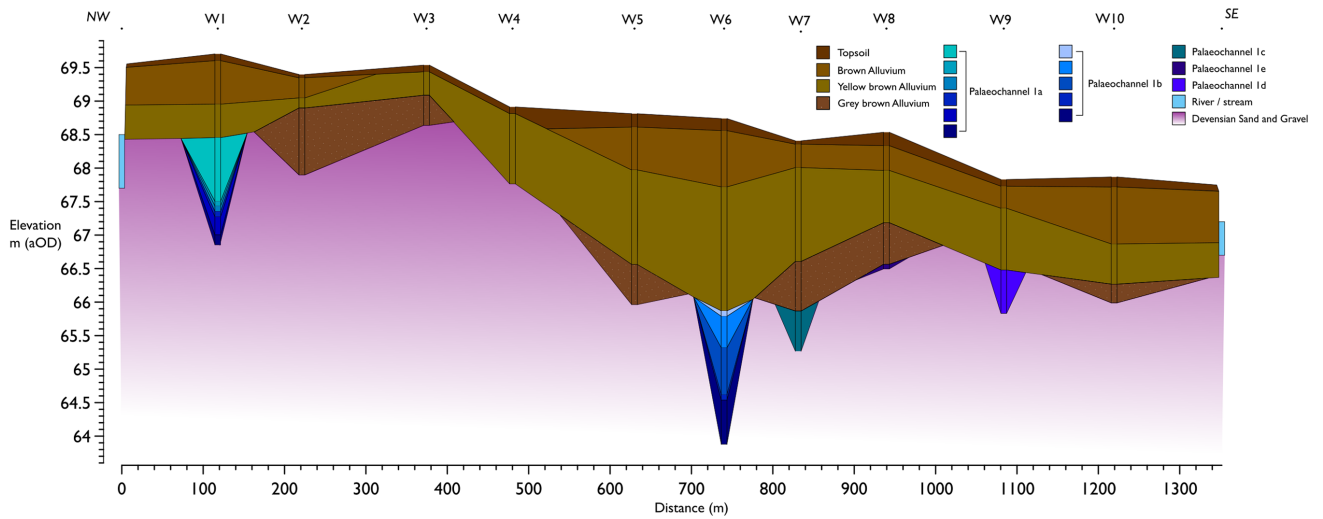
these deposits (Figure 10). However, in the south of the transect, there are numerous other palaeochannel deposits associated with narrower features that are poorly defined in the SAR imagery.

To the south of Court Farm, a series of more discrete paleochannels were apparent (**MW19**). As was suggested for Area MWb, these could be related to remnant of a former multichannel (anastomosing/braided) river.

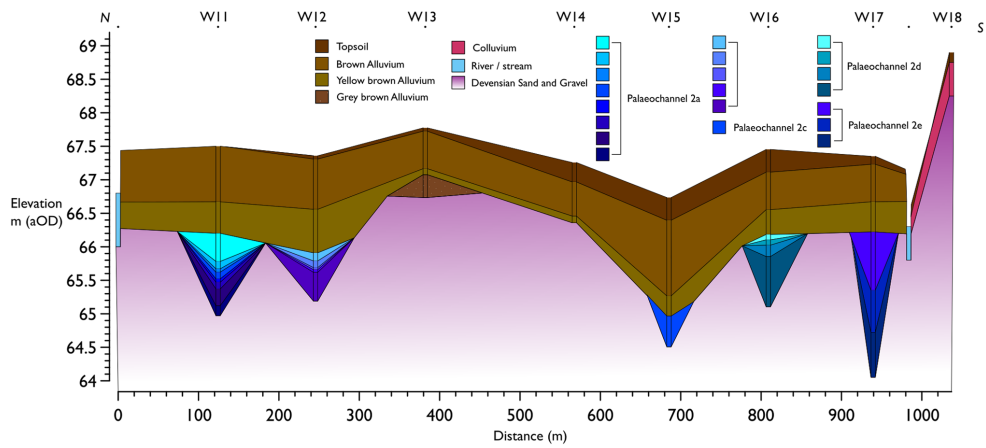
7 | Discussion

This study has captured and analysed a large volume of COSMO-SkyMed data within the valleys of the Rivers Lugg and Wye in Herefordshire (United Kingdom) and considered the most effective approach to displaying archaeologically significant landforms within a SAR time series. Although several approaches were considered, including the calculation of minimum, mean and maximum values, alongside data transformation methods such as PCA, due to the significant difference between the observed specular response of flooding and the more complex backscatter response of vegetation, these methods were mostly ineffective (see the [Supporting Information](#)). Thus, although the application of SAR time series data has previously enabled features that remain unchanged over time to be more clearly visualized (e.g., Cigna et al. 2014), this

Transect MWa



Transect MWb



Transect MWc

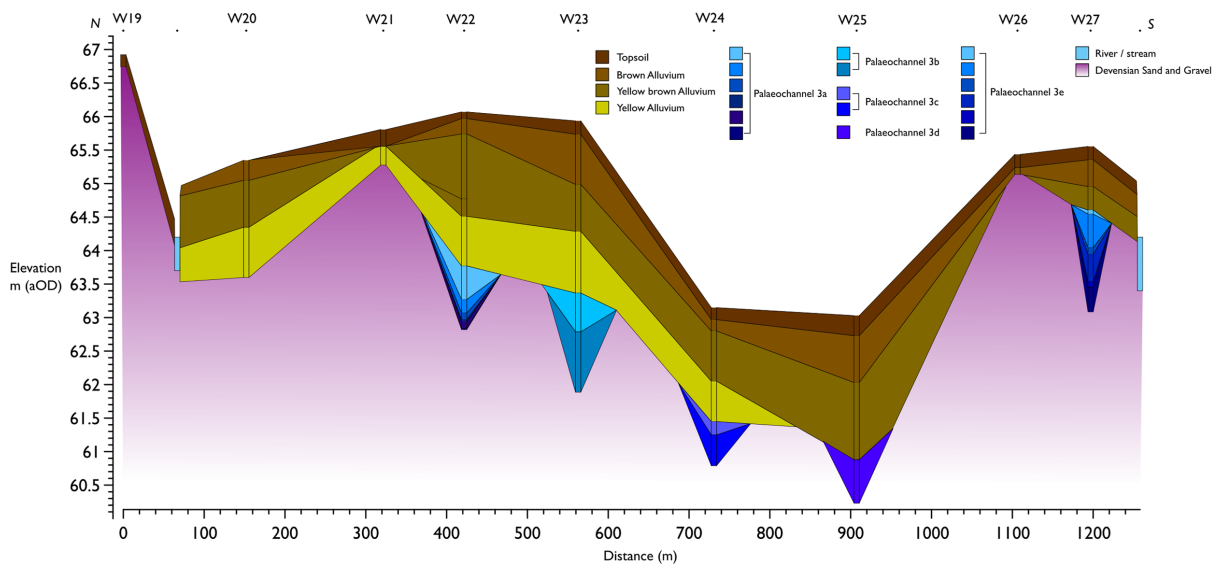


FIGURE 10 | Borehole Transects MWa, MWb and MWc (south facing) displayed at the same vertical and horizontal scale, with a consistent colour scheme pertaining to the observed sediment units.

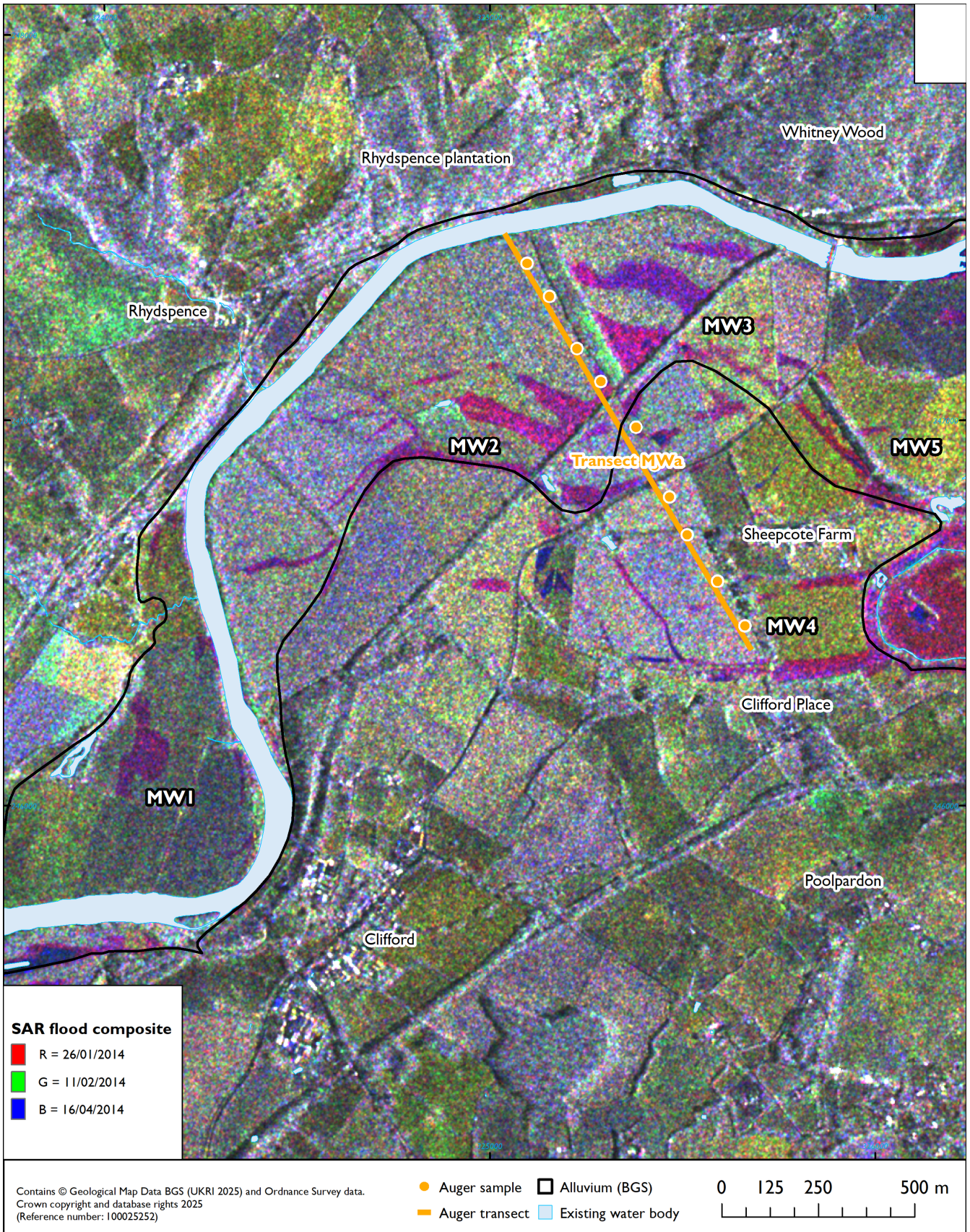


FIGURE 11 | SAR flood composite (Winter 2014) for Area MWa.

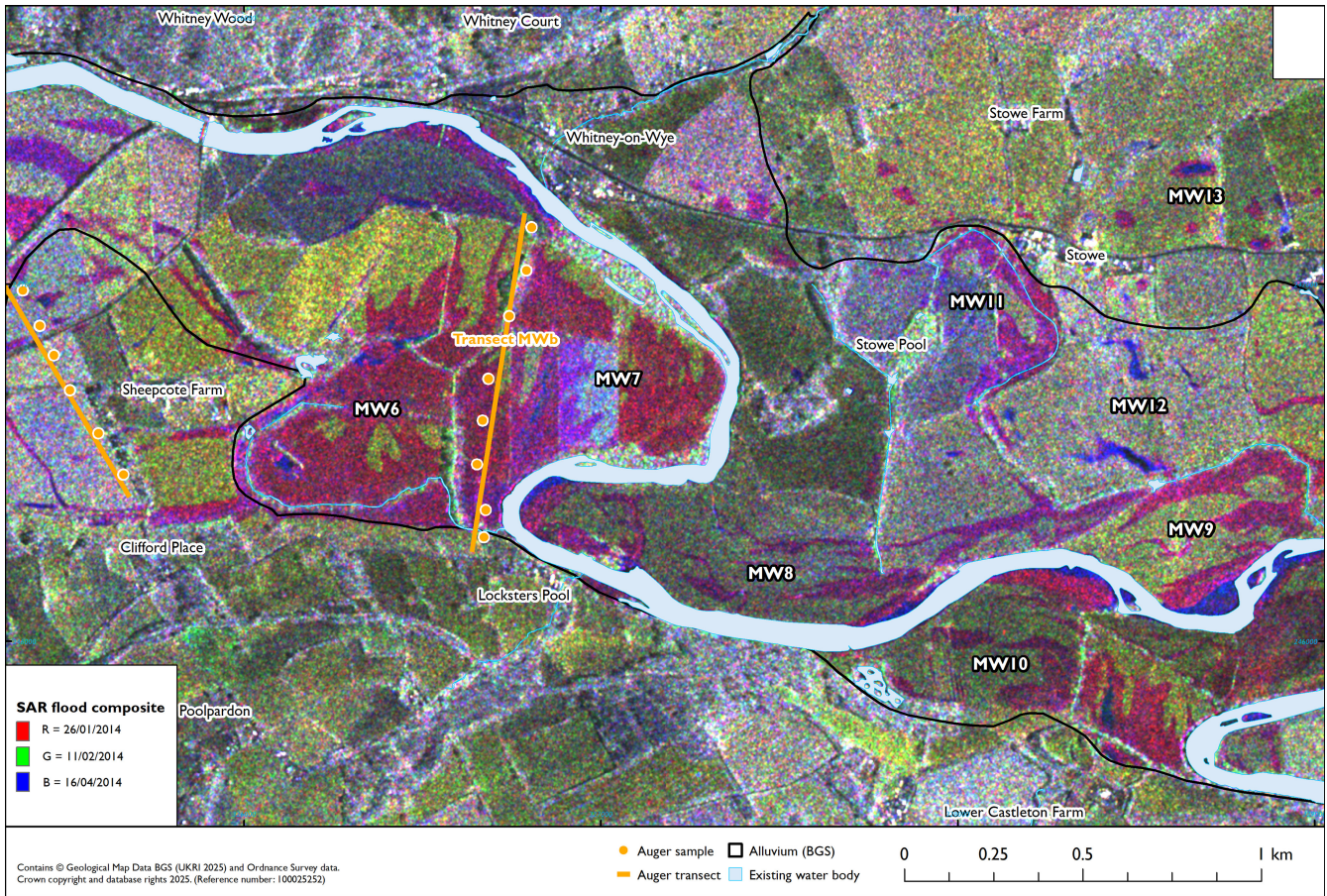


FIGURE 12 | SAR flood composite (Winter 2014) for Area MWb.

was challenging to implement in temperate floodplain environments where surface conditions can vary significantly throughout a year. Moreover, these data enhancements produced less clear images than the relatively simple composite images covering high magnitude single flood episodes, even when the time series was split into flooded and nonflooded datasets. Thus, imagery comprising data from three dates covering a single flood episode in the winter of 2014 was utilized as the optimal approach and was subsequently used to construct a deposit model for each case study. These images effectively defined the extent of flooding as a proxy for subtle surface topographic variations but also helped to highlight areas that persistently flood, regardless of topography, which may be influenced by the presence of subsurface landforms that have a greater capacity to retain groundwater (e.g., organic-rich palaeochannels and swales).

Palaeochannels and lower topographic zones were identified as areas that readily flood and correlated with the deepest areas of alluvial deposition, in turn characterized by anoxic conditions in the auger core transects. Similarly, higher topographic zones (e.g., gravel islands, bars and terrace remnants) were identified by areas that were not regularly covered by floodwater in the SAR data. These areas were found to relate to those characterized by thinner alluvial sediments in the auger transects. Thus, beyond defining the lateral (surface) extent of landforms, the application of SAR can provide proxy

indications of the depth and character of the underlying alluvial sedimentary sequence; therefore, SAR has extremely high potential for geoarchaeological investigations of alluvial environments.

Although SAR has enabled links to be made between surface expressions of landforms to subsurface sediment architecture in each case study area, it has not been possible to establish specific, quantitative relationships between sediment composition and backscatter response. For instance, textural and compositional differences in the alluvial sediment sequence are not directly observable, and the full complexity of the alluvial sediment sequence cannot be detailed from SAR alone. Nonetheless, a more holistic (large scale) understanding of landscape evolution has been achieved by linking remote sensing data with auger core records, which could be extended using borehole studies and other geotechnical datasets. This suggests that, when used synergistically, SAR data together with other datasets can provide a robust characterization of alluvial landforms, which has clear advantages in areas where blanket (Holocene) alluviation has predominated, such as the temperate river floodplains that occur widely in the United Kingdom and northwest Europe (Howard et al. 2015). Despite this, it was not possible in this study to clearly delineate valley floor landforms in SAR imagery where flooding was not present. This is because the shorter wavelengths provided by X-band SAR systems such as COSMO-SkyMed are unlikely

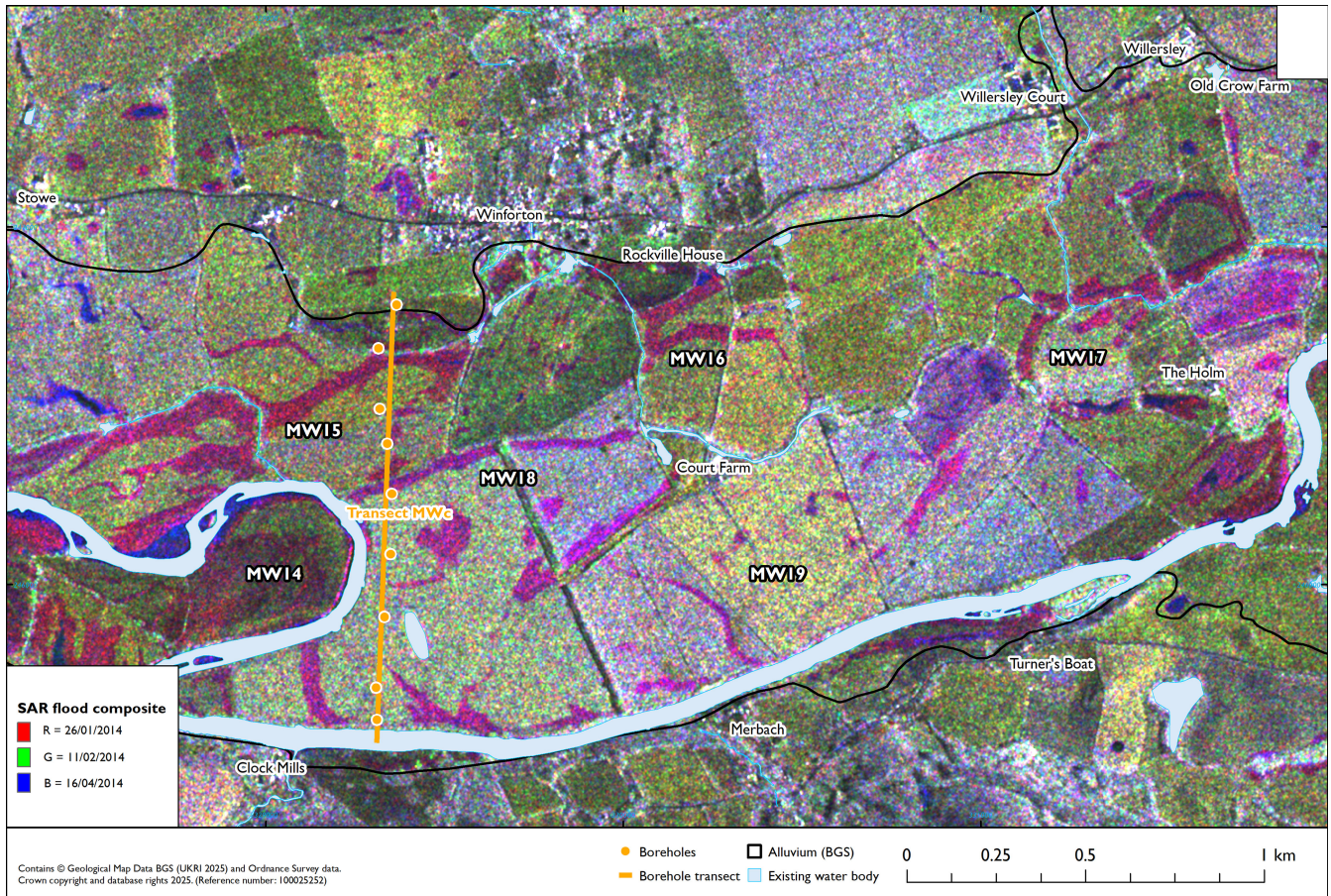


FIGURE 13 | SAR flood composite (Winter 2014) for Area MWa.

to penetrate the (vegetated) surface sufficiently to measure specific sediment characteristics (e.g., particle size). However, other lower frequency systems (e.g., L band) do have potential to provide such information, particularly in areas of bare soil. Consequently, the development of publicly accessible, higher resolution (2- to 8-m resolution) L-band data from systems such as the joint NASA/Indian Space Research Organization SAR (NISAR) mission may provide further opportunities for research in the future, particularly if this is combined with high temporal coverage (NASA 2024a).

The use of remote sensing techniques in a deposit modelling context is not a new area of research but has been limited to the application of passive datasets (e.g., aerial photography) and lidar (Baker 2003, 2007; Challis, Kincey, and Howard 2009; French, Macklin, and Passmore 1992; Lambrick 1992). However, as they become available, it is important that geoarchaeologists continue to explore the potential of other remote sensing datasets and evaluate the data gains they provide. Although this paper has demonstrated the potential of SAR, a comparison of this with the wider suite of remote sensing techniques available (e.g., lidar and multi/hyperspectral imagery) is still required to establish their full capability and contribution to both investigating and preserving these rich archaeological landscapes. Such analysis will allow for an improved understanding of the toolkit available for the reconstruction and mapping of archaeological resources in complex depositional settings such as alluvial environments.

8 | Conclusion

This investigation of portions of the Lugg and Wye floodplains in Herefordshire (United Kingdom) has demonstrated that, through the observation of contemporary episodes of flooding, SAR can facilitate an understanding of subsurface complexity across temperate alluvial environments. This was achieved through the selective analysis of images in a SAR (COSMO-SkyMed) time series, which provided a reliable and detailed representation of alluvial landforms such as palaeochannels and higher/lower topographic zones (e.g., gravel islands and terraces). The distribution of these landforms can, in turn, facilitate interpretation of their complexity and likely preservation capacity, leading to a greater understanding of landscape evolution, and associated distribution of archaeological resources. This information gain is highly beneficial in a deposit modelling framework, as it provides an opportunity to devise a more informed baseline, from which further geoarchaeological research questions can be directed. However, as most of the landforms delineated by SAR were established on the basis of the extent of contemporary flooding as a proxy for subtle surface topographic variations, higher resolution topographic datasets (e.g., lidar) will likely often be more effective. Despite this, in regions where such datasets are not available, SAR can provide a highly effective alternative, particularly given that these datasets can be low cost and cover large areas. In addition, features that persistently flood independent of topography, which are potentially influenced by the presence of other subsurface landforms (such

as any palaeochannels or lower lying topographic zones that are not expressed topographically), may be established, but to evaluate this capacity further, more detailed comparison between lidar and SAR is required.

As the goal of geoarchaeological research within alluvial environments is to understand human activity and its effects on hydrology and sedimentation patterns, the apogee of remote sensing would be the advancement of methods that can enable a detailed characterization of alluvial sediments. Although the SAR dataset used in this research does not presently allow for such definitions, there is potential for future systems to detail sediment characteristics such as particle size. This could allow for the consideration of sediment provenance and sediment supply, in turn helping to address issues of human impact upon river floodplains and other landscapes. Thus, geoarchaeologists must continue to explore the potential of remote sensing methods, and this research represents a step towards achieving this. Moreover, as the resources available to investigate temperate alluvial settings are often insufficient compared to the scale, complexity and archaeological richness of these landscapes, the promotion of SAR and other nonintrusive methods that are more compatible with conservation ethics and broader values of sustainability is highly desirable.

Acknowledgements

This work formed part of the main author's PhD research, which was supported by the UK's Engineering and Physical Sciences Research Council (EPSRC) grant for the Centre for Doctoral Training: Science and Engineering in Art, Heritage, and Archaeology (SEAHA; EP/L016036/1). The remote sensing data were acquired through the COSMO-SkyMed Constellation (Open Call for Science https://www.asi.it/bandi_e_concorsi/open-call-for-science-data-utilization-of-the-cosmo-skymed-mission-first-and-second-generation-english-versions/). The authors are grateful to Dr. Deodato Tapete (Agenzia Spaziale Italiana) for initial discussions on accessing the data from ASI and Dr. Niall Burnside (Scottish Association for Marine Science) and Robin Jackson (Worcestershire Archaeology) for their assistance with other aspects of this research. We would also like to thank colleagues, family and friends, particularly those who assisted in the auger sampling data for this research, in particular to Richard Higham, Megan Birtwhistle, Simon Walden, James Crabb and Eliza Crabb.

Conflicts of Interest

The authors declare no conflicts of interest.

Data Availability Statement

The data that support the findings of this study are available from Agenzia Spaziale Italiana, which can be acquired through the COSMO-SkyMed Constellation—Open Call for Science.

References

- Adams, A. R. E. W., W. E. Brown, and T. P. Culbert. 1981. "Radar Mapping, Archeology and Ancient Maya Land Use." *Science* 213, no. 4515: 1457–1463.
- Agenzia Spaziale Italiana. 2015. "Open Call for National and International Scientific Community." https://www.asi.it/bandi_e_concorsi/COSMO-SkyMed-constellation-data-utilization/.

Ager, T. 2021. *The Essentials of SAR: A Conceptual View of Synthetic Aperture Radar and Its Remarkable Capabilities*. Independently Published.

Amitrano, D., G. di Martino, A. Simone, and P. Imperatore. 2024. "Flood Detection With SAR: A Review of Techniques and Datasets." *Remote Sensing* 16, no. 4: 656. <https://doi.org/10.3390/rs16040656>.

Arnold, G., and R. Jackson. 2015. *Archaeological Salvage Recording at Wellington Quarry, Herefordshire 2014 Moreton South Extension: Phase 2a Interim Report*. Worcestershire Archaeology.

Arnold, G., and R. Jackson. 2016. *Archaeological Salvage Recording at Wellington Quarry, Herefordshire 2016 Moreton South Extension: Phase 2b + 2c (Part 1) Interim Report (Issue March 2017)*. Worcestershire Archaeology.

Ayala, G., J. Wainwright, J. Walker, et al. 2017. "Palaeoenvironmental Reconstruction of the Alluvial Landscape of Neolithic Çatalhöyük, Central Southern Turkey: The Implications for Early Agriculture and Responses to Environmental Change." *Journal of Archaeological Science* 87: 30–43. <https://doi.org/10.1016/j.jas.2017.09.002>.

Baghdadi, N., M. el Hajj, P. Dubois-Fernandez, M. Zribi, G. Belaud, and B. Cheviron. 2015. "Signal Level Comparison Between terraSAR-X and COSMO-SkyMed SAR Sensors." *IEEE Geoscience and Remote Sensing Letters* 12, no. 3: 448–452. <https://doi.org/10.1109/LGRS.2014.2342733>.

Baker, S. 2003. *The Trent Valley: Palaeochannel Mapping From Aerial Photographs*. Trent Valley Geoarchaeology Research Report. Trent & Peak Archaeology.

Baker, S. 2007. "The Palaeochannel Record in the Trent Valley UK: Contributions Towards Cultural Heritage Management." *Internet Archaeology* 20, no. 20. <https://doi.org/10.11141/ia.20.3>.

Bates, C. R., and M. R. Bates. 2016. "Palaeogeographic Reconstruction in the Transition Zone: The Role of Geophysical Forward Modelling in Ground Investigation Surveys." *Archaeological Prospection* 23, no. 4: 311–323. <https://doi.org/10.1002/arp.1546>.

Berendsen, H. J. A., K. M. Cohen, and E. Stouthamer. 2007. "The Use of GIS in Reconstructing the Holocene Palaeogeography of the Rhine-Meuse Delta, the Netherlands." *International Journal of Geographical Information Science* 21, no. 5: 589–602. <https://doi.org/10.1080/13658810601064918>.

Berendsen, H. J. A., and K. P. Volleberg. 2007. "New Prospects in Geomorphological and Geological Mapping of the Rhine-Meuse Delta—Application of Detailed Digital Elevation Maps Based on Laser Altimetry." *Netherlands Journal of Geosciences* 86, no. 1: 15–22. <https://doi.org/10.1017/S0016774600021296>.

Biondi, F. 2018. "COSMO-SkyMed High Resolution Fully Polarimetric Synthetic Aperture Radar Exploitation—The 'Strip-Spot' Approach." *International Journal of Remote Sensing* 39, no. 12: 3828–3838. <https://doi.org/10.1080/01431161.2018.1447163>.

Blickensdörfer, L., M. Schwieder, D. Pflugmacher, C. Nendel, S. Erasmí, and P. Hostert. 2022. "Mapping of Crop Types and Crop Sequences With Combined Time Series of Sentinel-1, Sentinel-2 and Landsat 8 Data for Germany." *Remote Sensing of Environment* 269: 112831.

Blom, R. G., R. E. Crippen, and C. Elachi. 1984. "Detection of Subsurface Features in Seasat Radar Images of Means Valley, Mojave Desert, California." *Geology* 12, no. 6: 346–349. [https://doi.org/10.1130/0091-7613\(1984\)12<346:DOSFIS>2.0.CO;2](https://doi.org/10.1130/0091-7613(1984)12<346:DOSFIS>2.0.CO;2).

Booth, P., A. Dodd, M. Robinson, and A. Smith. 2007. *The Archaeology of the Gravel Terraces of the Upper and Middle Thames: The Early Historical Period: AD1–1000: 27 (Illustrated Edition)*. Oxford University School of Archaeology.

Bradley, R. 2012. *An Archaeology of Natural Places*. Routledge. <https://doi.org/10.4324/9780203630228>.

- Brandon, A. 1989. *Geology of the Country Between Hereford and Leominster. Memoir for the 1:50 000 Geological Sheet 198 (England and Wales)*. British Geological Society.
- Brolly, M., and I. H. Woodhouse. 2012. "Vertical Backscatter Profile of Forests Predicted by a Macroecological Plant Model." *International Journal of Remote Sensing* 34, no. 4: 1026–1040. <https://doi.org/10.1080/01431161.2012.715777>.
- Brown, A. G. 1997. *Alluvial Geoarchaeology; Floodplain Archaeology and Environmental Change (Cambridge Manuals in Archaeology)*. Cambridge University Press.
- Bruniaux, G., M. Onfray, G. Dandurand, et al. 2024. "Thickness Estimation of the Soil-Sedimentary Cover Inside Causewayed Enclosures to Locate an Occupation Layer: Map of the Archaeological Potential of the Neolithic Causewayed Enclosure of Le Pontet." *Archaeological Prospection* 31, no. 2: 99–122. <https://doi.org/10.1002/arp.1934>.
- Brunning, R., and H. Chapman. 2013. *Somerset's Peatland Archaeology: Managing and Investigating a Fragile Resource*. Oxbow Books.
- Campana, S. 2017. "Remote Sensing in Archaeology." In *Encyclopaedia of Geoarchaeology*. Encyclopaedia of Earth Sciences, edited by A. Gilbert, with Associate Editors, P. Goldberg, V. Holliday, R. Mandel, and R. Sternberg, 703–725.
- Canti, M., J. Heathcote, G. Ayala, J. Corcoran, and J. Snidell. 2015. *Geoarchaeology. Using Earth Science to Understand the Archaeological Record*. Historic England.
- Carey, C., T. Brown, A. J. Howard, K. Challis, and L. Cooper. 2006. "Predictive Modelling of Multiperiod Geoarchaeological Resources at a River Confluence: A Case Study From the Trent-Soar, UK." *Archaeological Prospection* 13, no. 4: 241–250. <https://doi.org/10.1002/arp.295>.
- Carey, C., A. J. Howard, J. Corcoran, D. Knight, and J. Heathcote. 2019. "Deposit Modelling for Archaeological Projects: Methods, Practice, and Future Developments." *Geoarchaeology* 34, no. 4: 495–505. <https://doi.org/10.1002/gea.21712>.
- Carey, C., A. J. Howard, R. Jackson, and A. Brown. 2017. "Using Geoarchaeological Deposit Modelling as a Framework for Archaeological Evaluation and Mitigation in Alluvial Environments." *Journal of Archaeological Science: Reports* 11, no. February: 658–673. <https://doi.org/10.1016/j.jasrep.2017.01.013>.
- Carey, C., A. J. Howard, D. Knight, J. Corcoran, and J. Heathcote. 2018. *Deposit Modelling and Archaeology*. Shortrun Press.
- Carmichael, B., C. Daly, S. Fatorić, M. Macklin, S. McIntyre-Tamwoy, and W. Pittungnapoo. 2023. "Global Riverine Archaeology and Cultural Heritage: Flood-Risk Management and Adaptation for the Anthropogenic Climate Change Crisis." *Climate* 11, no. 10: 197. <https://doi.org/10.3390/cli11100197>.
- Challis, K., C. Carey, M. Kincey, and A. J. Howard. 2009. "Airborne Lidar Intensity and Geoarchaeological Prospection in River Valley Floors." *Archaeological Prospection* 18: 1–13. <https://doi.org/10.1002/arp.398>.
- Challis, K., M. Kincey, and A. J. Howard. 2009. "Airborne Remote Sensing of Valley Floor Geoarchaeology Using Daedalus ATM and CASI." *Archaeological Prospection* 16: 17–33. <https://doi.org/10.1002/arp.340>.
- Champness, C. 2018. "Bexhill to Hastings Link Road, East Sussex: A Geoarchaeological Deposit Model on the Combe Haven and Surrounding Valley Sequences." In *Deposit Modelling in Archaeology*, 53–66. Short Run Press.
- Chang-an, L., Z. Chen, Y. Shao, J. Chen, T. Hasi, and H. Pan. 2019. "Research Advances of SAR Remote Sensing for Agriculture Applications: A Review." *Journal of Integrative Agriculture* 18, no. 3: 506–525. [https://doi.org/10.1016/S2095-3119\(18\)62016-7](https://doi.org/10.1016/S2095-3119(18)62016-7).
- Chapman, B., and R. Blom. 2013. "Synthetic Aperture Radar, Technology, Past and Future Applications to Archaeology." In *Mapping Archaeological Landscapes From Space*, edited by D. C. Comer, M. J. Harrower, D. C. Comer, and M. J. Harrower, 113–132. Springer.
- Chen, F., H. Guo, D. Tapete, et al. 2022. "The Role of Imaging Radar in Cultural Heritage: From Technologies to Applications." *International Journal of Applied Earth Observation and Geoinformation* 112: 102907. <https://doi.org/10.1016/j.jag.2022.102907>.
- Chen, F., A. Jiang, P. Tang, et al. 2017. "Multi-Scale Synthetic Aperture Radar Remote Sensing for Archaeological Prospection in Han Hangu Pass, Xin'an China." *Remote Sensing Letters* 8, no. 1: 38–47. <https://doi.org/10.1080/2150704X.2016.1235812>.
- Chen, F., R. Lasaponara, and N. Masini. 2017. "An Overview of Satellite Synthetic Aperture Radar Remote Sensing in Archaeology: From Site Detection to Monitoring." *Journal of Cultural Heritage* 23: 5–11. <https://doi.org/10.1016/j.culher.2015.05.003>.
- Chen, F., N. Masini, J. Liu, J. You, and R. Lasaponara. 2016. "Multi-Frequency Satellite Radar Imaging of Cultural Heritage: The Case Studies of the Yumen Frontier Pass and Niya Ruins in the Western Regions of the Silk Road Corridor." *International Journal of Digital Earth* 9, no. 12: 1224–1241. <https://doi.org/10.1080/17538947.2016.1181213>.
- Chen, F., N. Masini, R. Yang, P. Milillo, D. Feng, and R. Lasaponara. 2015. "A Space View of Radar Archaeological Marks: First Applications of COSMO-SkyMed X-Band Data." *Remote Sensing* 7, no. 1: 24–50. <https://doi.org/10.3390/rs70100024>.
- Chiverrell, R. C., G. S. P. Thomas, and G. C. Foster. 2008. "Sediment-Landform Assemblages and Digital Elevation Data: Testing an Improved Methodology for the Assessment of Sand and Gravel Aggregate Resources in North-Western Britain." *Engineering Geology* 99, no. 1: 40–50. <https://doi.org/10.1016/j.enggeo.2008.02.005>.
- Chuvieco, E. 2020. *Fundamentals of Satellite Remote Sensing: An Environmental Approach*. 3rd ed. CRC Press. <https://doi.org/10.1201/9780429506482>.
- Cigna, F., T. Balz, D. Tapete, et al. 2023. "Exploiting Satellite SAR for Archaeological Prospection and Heritage Site Protection." *Geo-Spatial Information Science* 27, no. 3: 526–551. <https://doi.org/10.1080/10095020.2023.2223603>.
- Cigna, F., R. Lasaponara, N. Masini, P. Milillo, and D. Tapete. 2014. "Persistent Scatterer Interferometry Processing of COSMO-SkyMed Stripmap HIMAGE Time Series to Depict Deformation of the Historic Centre of Rome, Italy." *Remote Sensing* 6, no. 12: 12593–12618. <https://doi.org/10.3390/rs61212593>.
- Conesa, F. C., N. Devanthéry, A. L. Balbo, M. Madella, and O. Monserrat. 2014. "Use of Satellite SAR for Understanding Long-Term Human Occupation Dynamics in the Monsoonal Semi-Arid Plains of North Gujarat, India." *Remote Sensing* 6, no. 11: 11420–11443. <https://doi.org/10.3390/rs6111420>.
- Covello, f., F. Battazza, A. Coletta, et al. 2010. "COSMO-SkyMed an Existing Opportunity for Observing the Earth." *Journal of Geodynamics* 49, no. 3–4: 171–180. <https://doi.org/10.1016/j.jog.2010.01.001>.
- Crabb, N., C. Carey, A. J. Howard, and M. Brolly. 2023. "Lidar Visualization Techniques for the Construction of Geoarchaeological Deposit Models: An Overview and Evaluation in Alluvial Environments." *Geoarchaeology* 38, no. 4: 420–444. <https://doi.org/10.1002/gea.21959>.
- Crabb, N., C. Carey, A. J. Howard, R. Jackson, N. Burnside, and M. Brolly. 2022. "Modelling Geoarchaeological Resources in Temperate Alluvial Environments: The Capability of Higher Resolution Satellite Remote Sensing Techniques." *Journal of Archaeological Science* 141: 105576. <https://doi.org/10.1016/j.jas.2022.105576>.
- Dore, N., J. Patruno, E. Pottier, and M. Crespi. 2013. "New Research in Polarimetric SAR Technique for Archaeological Purposes Using ALOS

- PALSAR Data." *Archaeological Prospection* 20, no. 2: 79–87. <https://doi.org/10.1002/arp.1446>.
- Dorling, P. 2007. *The Lugg Valley, Herefordshire: Archaeology, Landscape, Change and Conservation*. Orphans Press.
- el Hajj, M., N. Baghdadi, M. Zribi, et al. 2016. "Soil Moisture Retrieval Over Irrigated Grassland Using X-Band SAR Data." *Remote Sensing of Environment* 176: 202–218. <https://doi.org/10.1016/j.rse.2016.01.027>.
- Elfadaly, A., N. Abate, N. Masini, and R. Lasaponara. 2020. "SAR Sentinel 1 Imaging and Detection of Palaeo-Landscape Features in the Mediterranean Area." *Remote Sensing* 12, no. 16: 2611. <https://doi.org/10.3390/rs12162611>.
- Engel, M., F. Henselowsky, F. Roth, et al. 2022. "Fluvial Activity of the Late-Glacial to Holocene "Bergstraßenneckar" in the Upper Rhine Graben Near Heidelberg, Germany—First Results." *Quaternary Science Journal* 71, no. 2: 213–226. <https://doi.org/10.5194/egqsj-71-213-2022>.
- Erasmı, S., R. Rosenbauer, R. Buchbach, T. Busche, and S. Rutishauser. 2014. "Evaluating the Quality and Accuracy of TanDEM-X Digital Elevation Models at Archaeological Sites in the Cilician Plain, Turkey." *Remote Sensing* 6, no. 10: 9475–9493. <https://doi.org/10.3390/rs6109475>.
- ESRI. 2024. "Interpretation of SAR Data for Flood Mapping—ArcGIS Pro/Documentation." <https://pro.arcgis.com/en/pro-app/latest/help/analysis/image-analyst/interpret-sar-data-for-flood-mapping.htm>.
- Evans, C., J. Tabor, and M. Vander Linden. 2016. *Twice-Crossed River: Prehistoric and Palaeoenvironmental Investigations at Barleycroft Farm/Over, Cambridgeshire: III*. McDonald Institute for Archaeological Research.
- Fezer, F. 1971. "Photo Interpretation Applied to Geomorphology—A Review." *Photogrammetria* 27, no. 1: 7–53. [https://doi.org/10.1016/0031-8663\(71\)90006-8](https://doi.org/10.1016/0031-8663(71)90006-8).
- Foster, I., and J. Boardman. 2024. *The Rother Valley: A Short History of a Lowland English River Catchment and Prospects for Future Management*.
- Fluck, H., and M. Dawson. 2021. "Climate Change and the Historic Environment." *Historic Environment: Policy & Practice* 12, no. 3–4: 263–270. <https://doi.org/10.1080/17567505.2021.1990492>.
- Freihardt, J., and O. Frey. 2023. "Assessing Riverbank Erosion in Bangladesh Using Time Series of Sentinel-1 Radar Imagery in the Google Earth Engine." *Natural Hazards and Earth System Sciences* 23, no. 2: 751–770. <https://doi.org/10.5194/nhess-23-751-2023>.
- French, C., H. Lewis, R. Scaife, and M. Allen. 2005. "New Perspectives on Holocene Landscape Development in the Southern English Chalklands: The Upper Allen Valley, Cranborne Chase, Dorset." *Geoarchaeology* 20, no. 2: 109–134. <https://doi.org/10.1002/gea.20039>.
- French, C., M. Macklin, and D. G. Passmore. 1992. "Archaeology and Palaeochannels in the Lower Welland and Nene Valleys: Alluvial Archaeology at the Fen Edge, Eastern England." In *Alluvial Archaeology in Britain*, edited by S. Needham and M. Macklin. Oxbow Mono.
- Gade, M., J. Kohlus, and C. Kost. 2017. "SAR Imaging of Archaeological Sites on Intertidal Flats in the German Wadden Sea." *Geosciences* 7, no. 4: 1–14. <https://doi.org/10.3390/geosciences7040105>.
- Garrison, T. G., B. Chapman, S. Houston, E. Román, and J. L. Garrido López. 2011. "Discovering Ancient Maya Settlements Using Airborne Radar Elevation Data." *Journal of Archaeological Science* 38, no. 7: 1655–1662. <https://doi.org/10.1016/j.jas.2011.02.031>.
- Gorrab, A., M. Zribi, N. Baghdadi, Z. Lili-Chabaane, and B. Mougenot. 2014. "Multi-Frequency Analysis of Soil Moisture Vertical Heterogeneity Effect on Radar Backscatter." In *2014 1st International Conference on Advanced Technologies for Signal and Image Processing (ATSIP)*, 379–384. IEEE. <https://doi.org/10.1109/ATSIP.2014.6834640>.
- Grimaldi, S., J. Xu, Y. Li, V. R. N. Pauwels, and J. P. Walker. 2020. "Flood Mapping Under Vegetation Using Single SAR Acquisitions." *Remote Sensing of Environment* 237: 111582. <https://doi.org/10.1016/j.rse.2019.111582>.
- Guccione, M. J. 2008. "Impact of the Alluvial Style on the Geoarchaeology of Stream Valleys." *Geomorphology* 101, no. 1–2: 378–401. <https://doi.org/10.1016/j.geomorph.2008.06.003>.
- Gurney, S., T. Astin, and G. Griffiths. 2010. "Origin and Structure of Devensian Depressions at Letton, Herefordshire." *Mercian Geologist* 17, no. 3: 181–184. https://centaur.reading.ac.uk/7601/1/Gurney_et_al_2010.pdf.
- Hachemi, K., F. Grecu, G. Ioana-Toroimac, Ș. Grigorie-Omrani, A. Ozer, and C. Kuzucuoglu. 2021. "The Utility of Morphometric Parameters Extracted From SAR Radar Images in the Monitoring of the Dynamics of the Danube Island System, Giurgiu-Călărăși Sector, Romania." *International Journal of Design & Nature and Ecodynamics* 16, no. 1: 13–19. <https://doi.org/10.18280/ijdne.160103>.
- Haskins, N. 2010. "Book Review—A Field Guide to Geophysics in Archaeology." *Archaeological Prospection* 62, no. December 2009: 61–62. <https://doi.org/10.1002/arp>.
- Hein, A. 2003. *Processing of SAR Data: Fundamentals, Signal Processing, Interferometry*. Springer.
- Herefordshire Archaeology. 2015. "Enclosures, West of the Green, Wellington (Herefordshire, UK) Herefordshire Council." <https://www.herefordshire.gov.uk/her-search/monuments-search/search/Monument?ID=5523>.
- Hill, C. L. 2014. "Rivers: Environmental Archaeology." In *Encyclopedia of Global Archaeology*, edited by C. Smith, 6343–6351. Springer. https://doi.org/10.1007/978-1-4419-0465-2_904.
- Historic England. 2018. *Prehistoric and Romano-British Settlements With Structures: Introductions to Heritage Assets*. Historic England.
- Historic England. 2020. "Deposit Modelling and Archaeology Guidance for Mapping Buried Deposits."
- Historic England. 2024a. *Freen's Court Magnate's Residence, Moat and Fishponds, Sutton St Michael, Sutton—1010392*. Historic England. <https://historicengland.org.uk/listing/the-list/list-entry/1010392>.
- Historic England. 2024b. *The Wergins Stone, Sutton—1005346*. Historic England. <https://historicengland.org.uk/listing/the-list/list-entry/1005346>.
- Holcomb, D., and I. Shingray. 2007. "Imaging Radar in Archaeological Investigations: An Imaging Processing Perspective." In *Satellite Remote Sensing for Archaeology*, edited by J. Wiseman and F. El-Baz, 11–45. Springer.
- Hosfield, R., and C. Green, eds. 2013. *Quaternary History and Palaeolithic Archaeology in the Axe Valley at Broom, South West England*. Oxbow Books.
- Houben, P., M. Schmidt, B. Mauz, A. Stobbe, and A. Lang. 2013. "Asynchronous Holocene Colluvial and Alluvial Aggradation: A Matter of Hydrosedimentary Connectivity." *Holocene* 23, no. 4: 544–555. <https://doi.org/10.1177/0959683612463105>.
- Howard, A. J., A. G. Brown, C. J. Carey, et al. 2008. "Archaeological Resource Modelling in Temperate River Valleys: A Case Study From the Trent Valley, UK." *Antiquity* 82, no. 318: 1040–1054. <https://doi.org/10.1017/S0003598X00097763>.
- Howard, A. J., S. J. Kluiwing, M. Engel, and V. M. A. Heyvaert. 2015. "Geoarchaeological Records in Temperate European River Valleys: Quantifying the Resource, Assessing Its Potential and Managing Its Future." *Quaternary International* 367: 42–50. <https://doi.org/10.1016/j.quaint.2014.05.003>.
- Howard, A. J., T. J. Coulthard, and D. Knight. 2017. "The Potential Impact of Green Agendas on Historic River Landscapes: Numerical Modelling of Multiple Weir Removal in the Derwent Valley Mills World Heritage Site, UK." *Geomorphology* 293: 37–52.

- Jackson, R., T. G. Brown, C. Carey, et al. 2013. "Delivering the Benefits of Aggregates Levy Sustainability Funded Research on River Valley Archaeological Sites in the Severn-Wye Catchment, UK." *Historic Environment: Policy & Practice* 3, no. 2: 97–115. <https://doi.org/10.1179/1756750512z.0000000009>.
- Jackson, R., and D. Miller. 2011. *Wellington Quarry, Herefordshire (1986–96): Investigations of a Landscape in the Lower Lugg Valley*. Oxbow books.
- Jensen, J. R. 2007. *Remote Sensing of the Environment: An Earth Resource Perspective*. 2nd ed. Prentice Hall.
- Jiang, A., F. Chen, N. Masini, et al. 2017. "Archeological Crop Marks Identified From COSMO-SkyMed Time Series: The Case of Han-Wei Capital City, Luoyang, China." *International Journal of Digital Earth* 10, no. 8: 846–860. <https://doi.org/10.1080/17538947.2016.1254686>.
- Jones, A. F., A. F. Jones, P. A. Brewer, E. Johnstone, and M. G. Macklin. 2007. "High-Resolution Interpretative Geomorphological Mapping of River Valley Environments Using Airborne LiDAR Data." *Earth Surface Processes and Landforms* 1592, no. March: 1574–1592. <https://doi.org/10.1002/esp.1505>.
- Jones, H., and R. Vaughan. 2010. *Remote Sensing of Vegetation: Principles, Techniques, and Applications*. Oxford University Press.
- Khoshnevis, S. A., and S. Ghorshi. 2020. "A Tutorial on Tomographic Synthetic Aperture Radar Methods." *SN Applied Sciences* 2, no. 9: 1504. <https://doi.org/10.1007/s42452-020-03298-6>.
- Kiarszys, G., and A. I. Zaleska. 2017. "Sensing the Material Remains of the Forgotten Great War in Poland." *Sensibly or Sensationally—The Dilemma in Front of Presenting Results of the Airborne Laser Scanning Visualisations* 16: 101–116. <https://doi.org/10.1007/978-3-319-50518-3>.
- Kibblewhite, M., G. Tóth, and T. Hermann. 2015. "Predicting the Preservation of Cultural Artefacts and Buried Materials in Soil." *Science of the Total Environment* 529: 249–263. <https://doi.org/10.1016/j.scitotenv.2015.04.036>.
- Kumar, S., P. Siqueira, H. Govil, and S. Agrawal. 2023. *Spaceborne Synthetic Aperture Radar Remote Sensing: Techniques and Applications*. CRC Press.
- Lambrick, G. 1992. "Alluvial Archaeology of the Holocene in the Upper Thames Basin 1971–1991: A Review." In *Alluvial Archaeology in Britain*, edited by S. Needham and M. G. Macklin, 209–225. Oxbow Books.
- Lambrick, G., M. A. Robinson, and M. Wachnik. 2009. *The Thames Through Time: The Archaeology of the Grave Terraces of the Upper and Middle Thames: The Thames Valley in Late Prehistory, 1500 BC–AD 50*. Oxford Archaeology.
- Lasaponara, R., and N. Masini. 2012. "Image Enhancement, Feature Extraction and Geospatial Analysis in an Archaeological Perspective." In *Satellite Remote Sensing: A New Tool for Archaeology*, edited by R. Lasaponara and N. Masini, 17–64. Springer.
- Lasaponara, R., and N. Masini. 2013. "Satellite Synthetic Aperture Radar in Archaeology and Cultural Landscape: An Overview." *Archaeological Prospection* 20, no. 2: 71–78. <https://doi.org/10.1002/arp.1452>.
- Lasaponara, R., N. Masini, A. Pecci, et al. 2017. "Qualitative Evaluation of COSMO SkyMed in the Detection of Earthen Archaeological Remains: The Case of Pachamacac (Peru)." *Journal of Cultural Heritage* 23: 55–62. <https://doi.org/10.1016/j.culher.2015.12.010>.
- Lillesand, T. M., R. W. Kiefer, and J. W. Chipman. 2015. *Remote Sensing and Image Interpretation*. 7th ed. Wiley.
- Luo, L., X. Wang, H. Guo, et al. 2019. "Airborne and Spaceborne Remote Sensing for Archaeological and Cultural Heritage Applications: A Review of the Century (1907–2017)." *Remote Sensing of Environment* 232: 111280. <https://doi.org/10.1016/j.rse.2019.111280>.
- Malone, S. 2014. "Lincolnshire Fenland Lidar. Archaeological Project Services, Report No. 46/09."
- Matthiesen, H., R. Brunning, B. Carmichael, and J. Hollesen. 2022. "Wetland Archaeology and the Impact of Climate Change." *Antiquity* 96, no. 390: 1412–1426. <https://doi.org/10.15184/aqy.2022.112>.
- McHugh, W. P., G. G. Schaber, C. S. Breed, and J. F. McCauley. 1989. "Neolithic Adaptation and the Holocene Functioning of Tertiary Palaeodrainages in Southern Egypt and Northern Sudan." *Antiquity* 63, no. 239: 320–336. <https://doi.org/10.1017/S0003598X00076031>.
- Meyer, F. 2019. "Spaceborne Synthetic Aperture Radar: Principles, Data Access, and Basic Processing Techniques." In *The Synthetic Aperture Radar (SAR) Handbook: Comprehensive Methodologies for Forest Monitoring and Biomass Estimation*. NASA SERVIR Program.
- Meylemans, E., F. Bogemans, A. Storme, Y. Perdaen, I. Verdurmen, and K. Deforce. 2013. "Lateglacial and Holocene Fluvial Dynamics in the Lower Scheldt Basin (N-Belgium) and Their Impact on the Presence, Detection and Preservation Potential of the Archaeological Record." *Quaternary International* 308: 148–161. <https://doi.org/10.1016/j.quaint.2013.03.034>.
- Mitidieri, F., M. N. Papa, D. Amitrano, and G. Ruello. 2016. "River Morphology Monitoring Using Multitemporal SAR Data: Preliminary Results." *European Journal of Remote Sensing* 49, no. 1: 889–898. <https://doi.org/10.5721/EuJRS20164946>.
- Moore, E., A. Freeman, and S. Hensley. 2007. "Spaceborne and Airborne Radar at Ankgor: Introducing New Technology to the Ancient Site." In *Remote Sensing in Archaeology*, edited by J. Wiseman and F. El-Baz, 185–216. Springer.
- Morigi, T., D. Schreve, M. White, and G. Hey. 2011. *The Archaeology of the Gravel Terraces of the Upper and Middle Thames: Early Prehistory to 1500 BC (Illustrated Edition)*. Oxford University School of Archaeology.
- Nagel, G. W., S. E. Darby, and J. Leyland. 2023. "The Use of Satellite Remote Sensing for Exploring River Meander Migration." *Earth-Science Reviews* 247: 104607. <https://doi.org/10.1016/j.earscirev.2023.104607>.
- NASA. 2024a. *NASA-ISRO SAR Mission (NISAR): Mission Concept*. NASA-ISRO SAR Mission (NISAR). <https://nisar.jpl.nasa.gov/mission/mission-concept>.
- NASA. 2024b. "What Is Synthetic Aperture Radar?: Background Information on Synthetic Aperture Radar, With Details on Wavelength and Frequency, Polarization, Scattering Mechanisms, and Interferometry." <https://www.earthdata.nasa.gov/learn/backgrounders/what-is-sar>.
- Passmore, D. G., C. Waddington, and S. J. Houghton. 2002. "Geoarchaeology of the Milfield Basin, Northern England; Towards an Integrated Archaeological Prospection, Research and Management Framework." *Archaeological Prospection* 9, no. 2: 71–91. <https://doi.org/10.1002/arp.184>.
- Parag, M., R. Lottering, K. Peerbhay, N. Agjee, and N. Poona. 2024. "The Use of Synthetic Aperture Radar Technology for Crop Biomass Monitoring: A Systematic Review." *Remote Sensing Applications: Society and Environment* 33: 101107.
- Patrino, J., N. Dore, M. Crespi, and E. Pottier. 2013. "Polarimetric Multifrequency and Multi-Incidence SAR Sensors Analysis for Archaeological Purposes." *Archaeological Prospection* 20, no. 2: 89–96. <https://doi.org/10.1002/arp.1448>.
- Payne, R., and D. Jordan. 2011. "Geoarchaeology." In *Wellington Quarry, Herefordshire (1986–1996): Investigation in the Lower Lugg Valley*, 28–33. Oxbow Books.
- Pouquet, J. 1974. *Earth Sciences in the Age of the Satellite*. Springer Netherlands. <https://doi.org/10.1007/978-94-010-2188-3>.
- Rosenfeld, C. L. 1984. "Remote Sensing Techniques for Geomorphologists." In *Developments and Applications of Geomorphology*, edited by J. E. Costa and P. J. Fleisher, 1–37. Springer. https://doi.org/10.1007/978-3-642-69759-3_1.

- Rossi, D., G. Zolezzi, W. Bertoldi, and A. Vitti. 2023. "Monitoring Braided River-Bed Dynamics at the Sub-Event Time Scale Using Time Series of Sentinel-1 SAR Imagery." *Remote Sensing* 15, no. 14: 3622. <https://doi.org/10.3390/rs15143622>.
- Salisbury, C. 1984. "Flandrian Courses of the River Trent at Colwick, Nottingham." *Mercian Geologist* 9, no. 4: 189–207.
- Salisbury, C. 1992. "The Archaeological Evidence for Palaeochannels in the Trent Valley." In *Alluvial Archaeology in Britain*, 155–162. Oxbow Books (Oxbow Monograph, 27).
- Santi, E., G. Fontanelli, F. Montomoli, et al. 2012. "The Retrieval and Monitoring of Vegetation Parameters From COSMO-SkyMed Images." In *2012 IEEE International Geoscience and Remote Sensing Symposium*, 7031–7034. IEEE. <https://doi.org/10.1109/IGARSS.2012.6351952>.
- Short, N., and R. Blair. 1986. *Geomorphology From Space: A Global Overview of Regional Landforms*. NASA.
- Simms, E. L. 2020. *SAR Image Interpretation for Various Land Covers: A Practical Guide*. CRC Press.
- Stein, S., S. Malone, D. Knight, A. Howard, and C. Carey. 2017. "New Approaches to Mapping and Managing Palaeochannel Resources in the Light of Future Environmental Change: A Case Study From the Trent Valley, UK." *Historic Environment: Policy & Practice* 8, no. 2: 113–124. <https://doi.org/10.1080/17567505.2017.1317086>.
- Stewart, C. 2017. "Detection of Archaeological Residues in Vegetated Areas Using Satellite Synthetic Aperture Radar." *Remote Sensing* 9, no. 2: 118. <https://doi.org/10.3390/rs9020118>.
- Tapete, D., and F. Cigna. 2017. "Trends and Perspectives of Space-Borne SAR Remote Sensing for Archaeological Landscape and Cultural Heritage Applications." *Journal of Archaeological Science: Reports* 14: 716–726. <https://doi.org/10.1016/j.jasrep.2016.07.017>.
- Tapete, D., and F. Cigna. 2019. "COSMO-SkyMed SAR for Detection and Monitoring of Archaeological and Cultural Heritage Sites." *Remote Sensing* 11, no. 11: 1326. <https://doi.org/10.3390/rs11111326>.
- Tapete, D., F. Cigna, and D. N. M. Donoghue. 2016. "'Looting Marks' in Space-Borne SAR Imagery: Measuring Rates of Archaeological Looting in Apamea (Syria) With TerraSAR-X Staring Spotlight." *Remote Sensing of Environment* 178: 42–58. <https://doi.org/10.1016/j.rse.2016.02.055>.
- van de Noort, R., and A. O'Sullivan. 2006. *Rethinking Wetland Archaeology*. Duckworth.
- van der Meulen, B., K. M. Cohen, H. J. Pierik, J. J. Zinsmeister, and H. Middelkoop. 2020. "LiDAR-Derived High-Resolution Palaeo-DEM Construction Workflow and Application to the Early Medieval Lower Rhine Valley and Upper Delta." *Geomorphology* 370: 107370. <https://doi.org/10.1016/j.geomorph.2020.107370>.
- van Dinter, M., K. M. Cohen, W. Z. Hoek, E. Stouthamer, E. Jansma, and H. Middelkoop. 2017. "Late Holocene Lowland Fluvial Archives and Geoarchaeology: Utrecht's Case Study of Rhine River Abandonment Under Roman and Medieval Settlement." *Quaternary Science Reviews* 166: 227–265. <https://doi.org/10.1016/j.quascirev.2016.12.003>.
- Verhegge, J., T. Missiaen, and P. Crombé. 2016. "Exploring Integrated Geophysics and Geotechnics as a Paleolandscape Reconstruction Tool: Archaeological Prospection of (Prehistoric) Sites Buried Deeply Below the Scheldt Polders (NW Belgium)." *Archaeological Prospection* 23, no. 2: 125–145. <https://doi.org/10.1002/arp.1533>.
- Verhegge, J., A. Storme, F. Cruz, and P. Crombé. 2021. "Cone Penetration Testing for Extensive Mapping of Deeply Buried Late Glacial Coversand Landscape Paleotopography." *Geoarchaeology* 36, no. 1: 130–148. <https://doi.org/10.1002/gea.21815>.
- Watt, S. 2011. "The Archaeology of the West Midlands: A Framework for Research." In *The Archaeology of the West Midlands*. Oxbow books. <https://doi.org/10.2307/j.ctvh1ds40>.
- White, M., M. Bates, M. Pope, et al. 2016. *Lost Landscapes of Palaeolithic Britain: The Contribution of Projects Funded by the Aggregates Levy Sustainability Fund 2002–2011*. Oxford Archaeology.
- Wiseman, J., and F. El-Baz. 2007. *Remote Sensing in Archaeology (Interdisciplinary Contributions to Archaeology)*. Springer.

Supporting Information

Additional supporting information can be found online in the Supporting Information section.